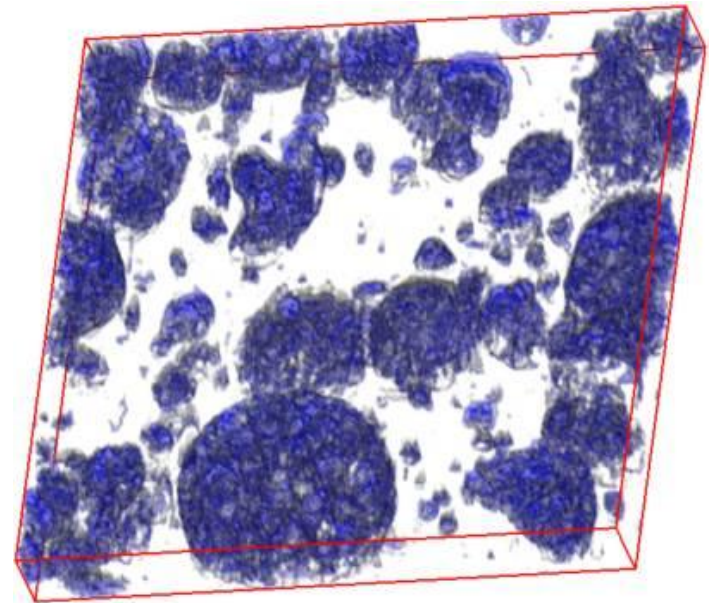
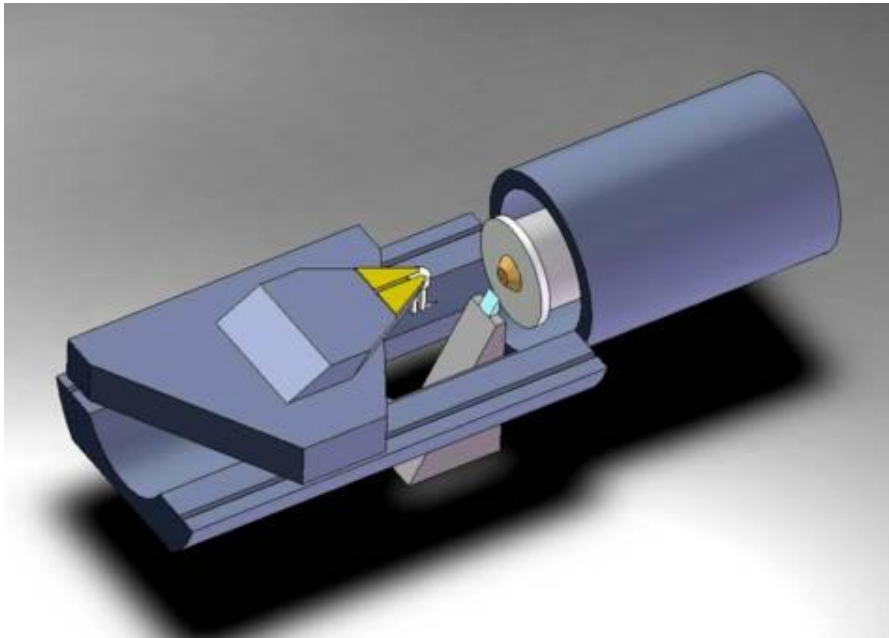


3D structure analysis of biomaterials by scanning probe nanotomography

A.E. Efimov, O.I. Agapova, I.I. Agapov,
Shumakov Federal Research Center of Transplantology and Artificial Organs



Scanning probe nanotomography – non-destructive three-dimensional analysis of native nanoscale structures in a wide range of soft materials.

The Solution is based on combination of

scanning probe microscopy (nanoscale analysis of surface features)

and

(Cryo)ultramicrotomy (ultrathin sectioning of soft materials at room temperature and low temperatures down to -190°C).

Background

Scanning probe microscopy

(surface analysis at nanoscale)

2D (XY)

+

Ultramicrotomy

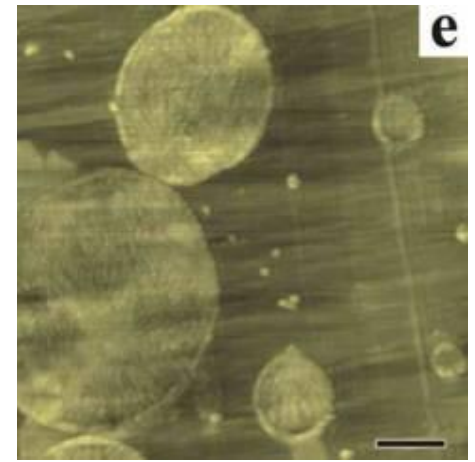
(ultrathin sectioning to 10 nm
At temperature from -190 to +20 C)

1D (Z)

=

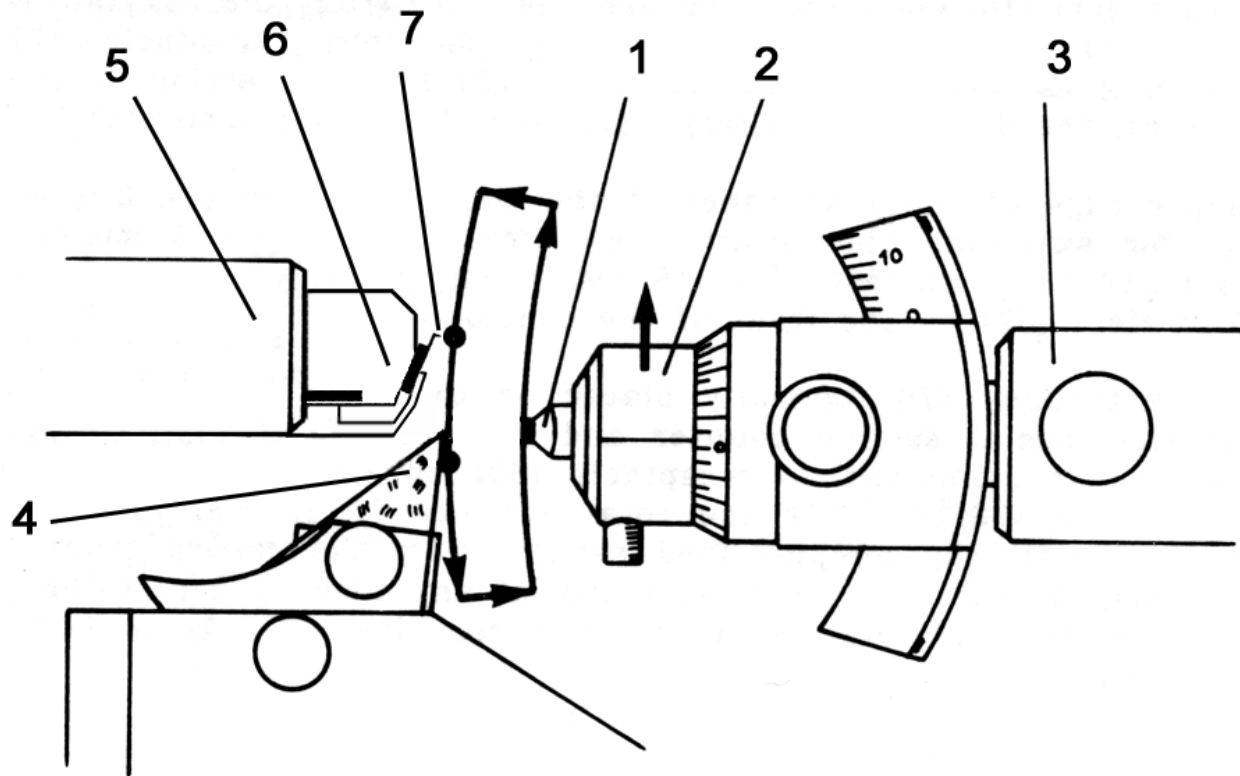
Scanning probe nanotomography

3D(XYZ)



CONCEPT: in situ AFM measurement of the blockface after ultramicrotome cutting in ambient and cryogenic conditions.

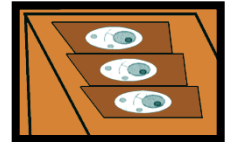
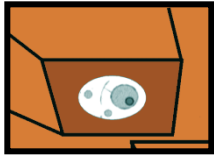
3D reconstruction by serial section/measurements with uniform section thickness.



Scheme of combination of SPM and ultramicrotome:

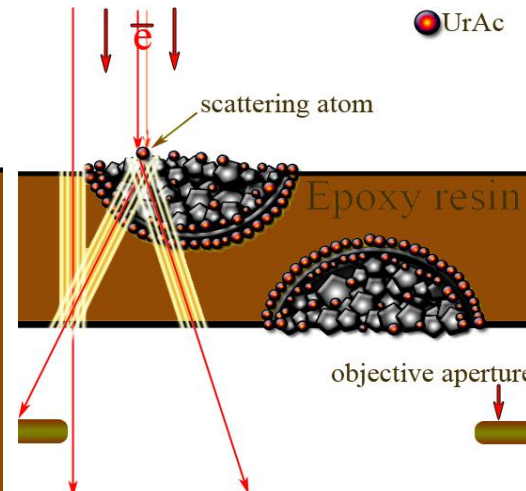
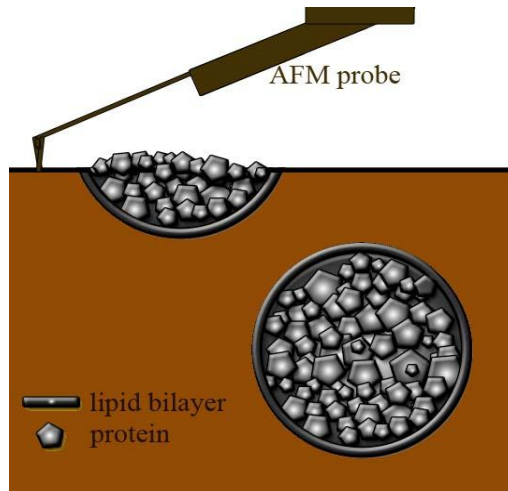
- 1 – sample,
- 2 – sample holder,
- 3 – moving ultramicrotome arm,
- 4 – ultramicrotome knife,
- 5 – SPM scanner,
- 6 – probe holder,
- 7 – SPM probe.

AFM and TEM image contrast formation



Block face

Ultrathin section
10-90nm



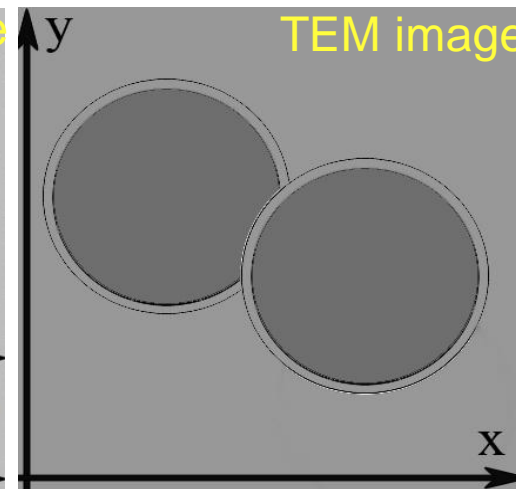
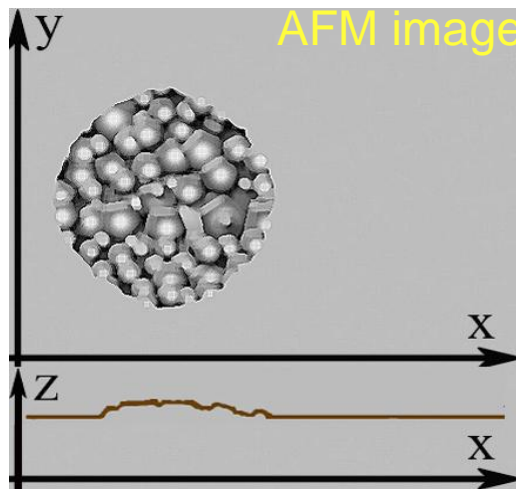
Vacuum
OR
gas/liquid
Environment

Surface
morphology;
Mechanical
and electrical
properties;

Data of molecular
(protein) content
from the surface.

Native structure
preservation

- Vacuum
- Electron beam
- Low contrast on polymer/bio unstained samples
- Projection imaging



The methods of nanostructure analysis(biology&polymers)

Product or Technology	Resolution		Cost	Preparation and damage to the sample structure
	XY, nm	Z, nm		
SPM + CryoUMT (SNOTRA)	5..10	10-20	~250 k\$	Intact native structures of soft polymers and biomaterials are measured (cryoultratomography and immediate measurement)
Conventional SPM, Bruker, Asylum, ...	5..10	No! Measures only the surface	~200 k\$	Structures are damaged (measurements at room temperature)
CryoSPM, Omicron, JEOL, ...	5..10		>300 k\$	Hard to exploit (vacuum, liquid He or N ₂ environment – not suited for bio/polymers)
SEM Tomography (Focused-ion-beam sectioning), FEI, Zeiss	10	~10-20	>600 k\$	Structures are damaged (electron and ion beams, vacuum, metal sputtering), no cryo 3D at the moment
CryoTEM (electronic tomography), FEI, Hitachi	5	5 Sample thickness <100 nm	> 1M\$	Structures are damaged (electron and ion beams, vacuum), projection imaging, low contrast at biological and polymer samples

1. Room temperature AFM + ultramicrotome



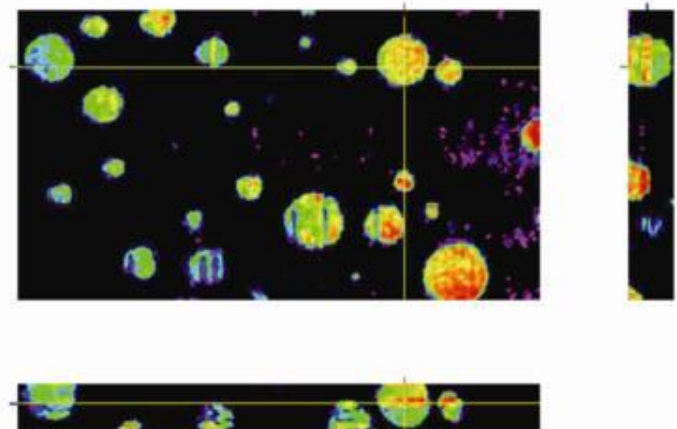
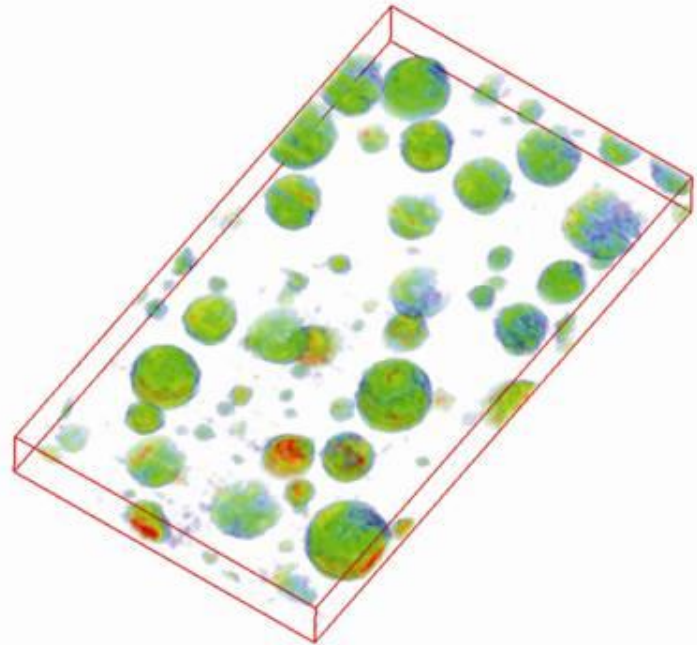
3D-AFM applications

3D model of polymer sample

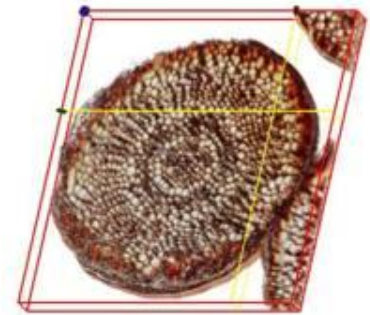
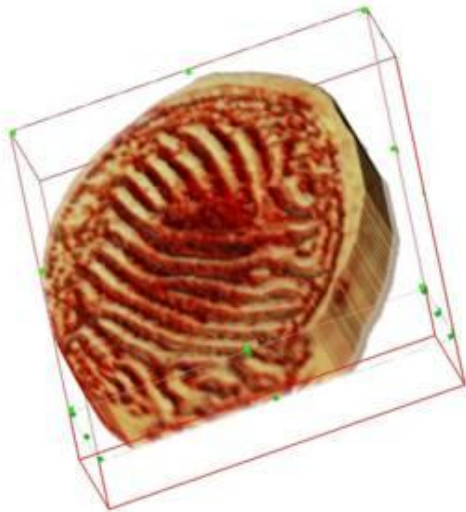
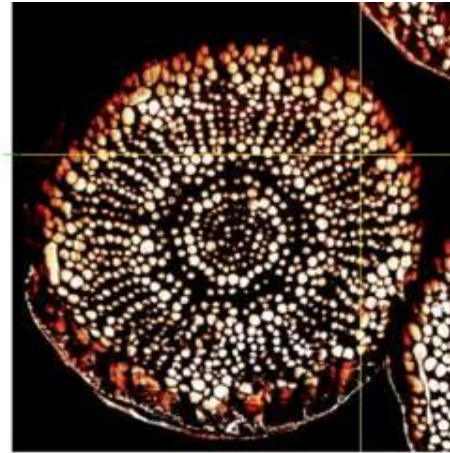
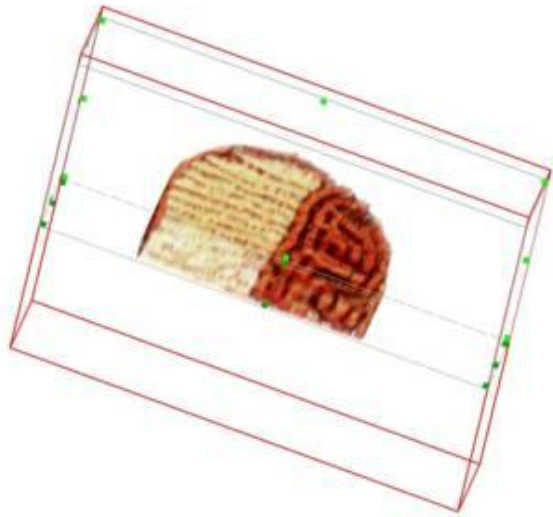
3D model of ABS/PA6 (Acrylonitrile-butadiene-styrene/polyamide6) polymer blend structure (8.75 5.0 1.0 μm , 25 sections, spaces between sections 40 nm).

Sample courtesy of Institut f. Polymere, ETH-Hönggerberg, Switzerland;

Journal of Microscopy, Vol. 226, Pt 3, 2007, pp. 207–217



Study of polymer and nanocomposite fibers

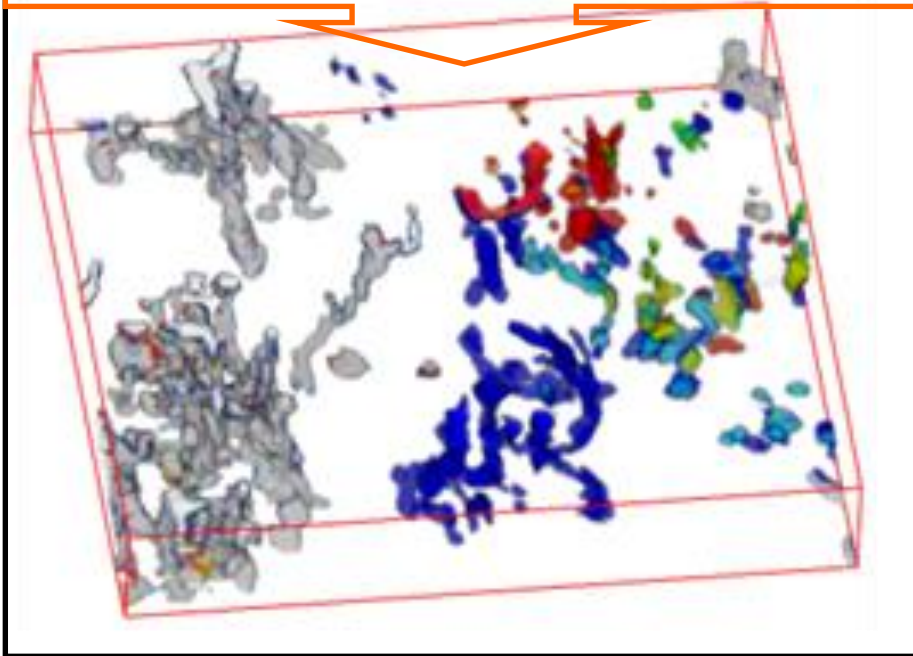


3D-reconstruction of carbon (left, $4.0 \times 4.0 \times 1.0 \mu\text{m}$) and polymer (PET/PE “islands-in-the-sea” fibers, $32 \times 32 \times 1.5 \mu\text{m}$) fibers, samples courtesy of Prof. J.P. Hinestrosa, **Cornell University**, USA

3D reconstruction of conductive nanocomposites

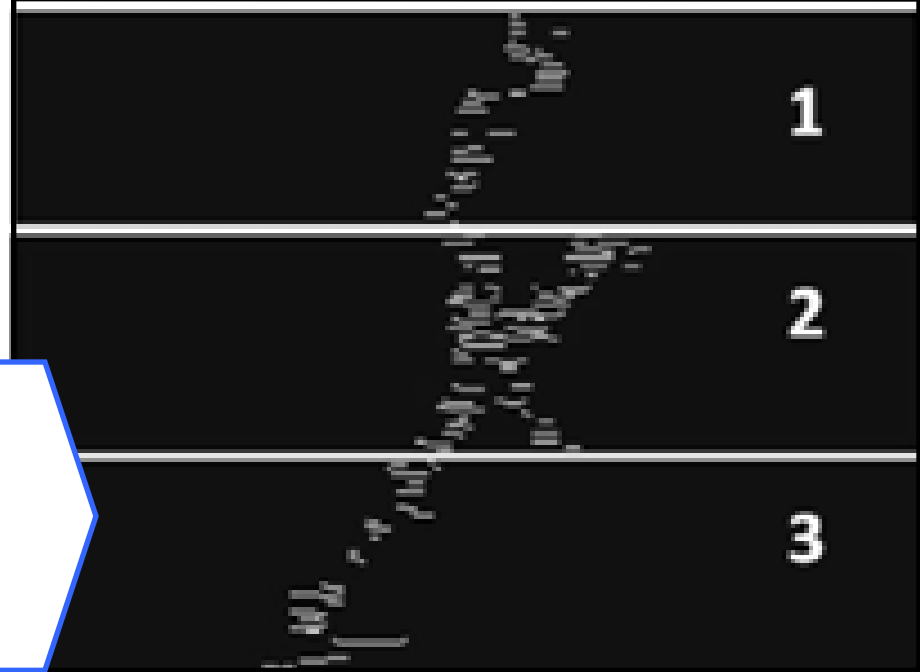
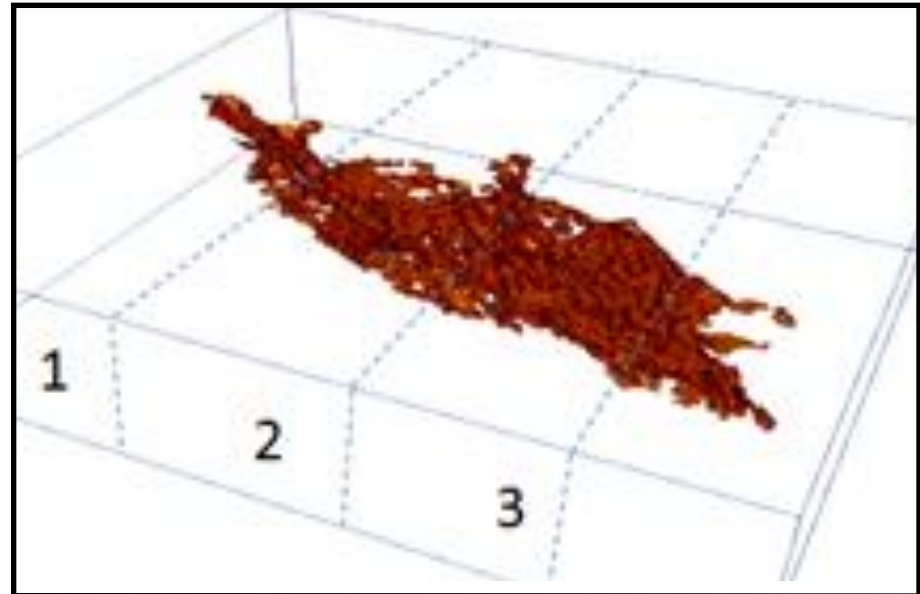
3D-reconstruction of conductive nanotube network in polystyrene/CNT, 1.8x1.6x0.26 μm , section thickness 12 nm.

A. Alekseev, A. Efimov, K. Lu, J. Loos, *Adv. Mater.*, 2009, 21, 4915

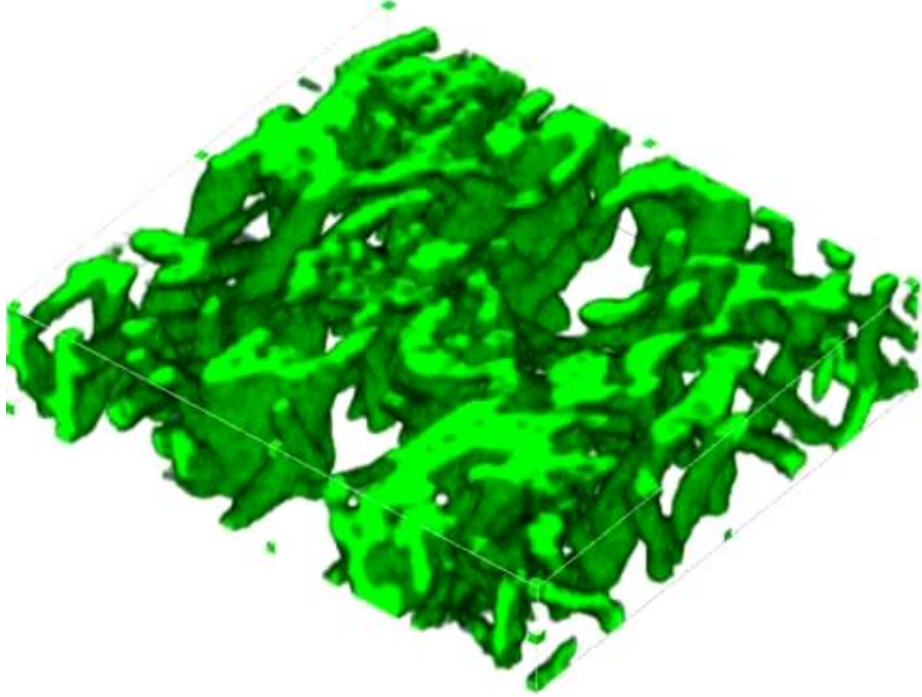


3D-reconstruction of conductive network of graphene clusters in polystyrene/graphene nanocomposite, 2.5x2.5x0.34 μm , section thickness 12 nm.

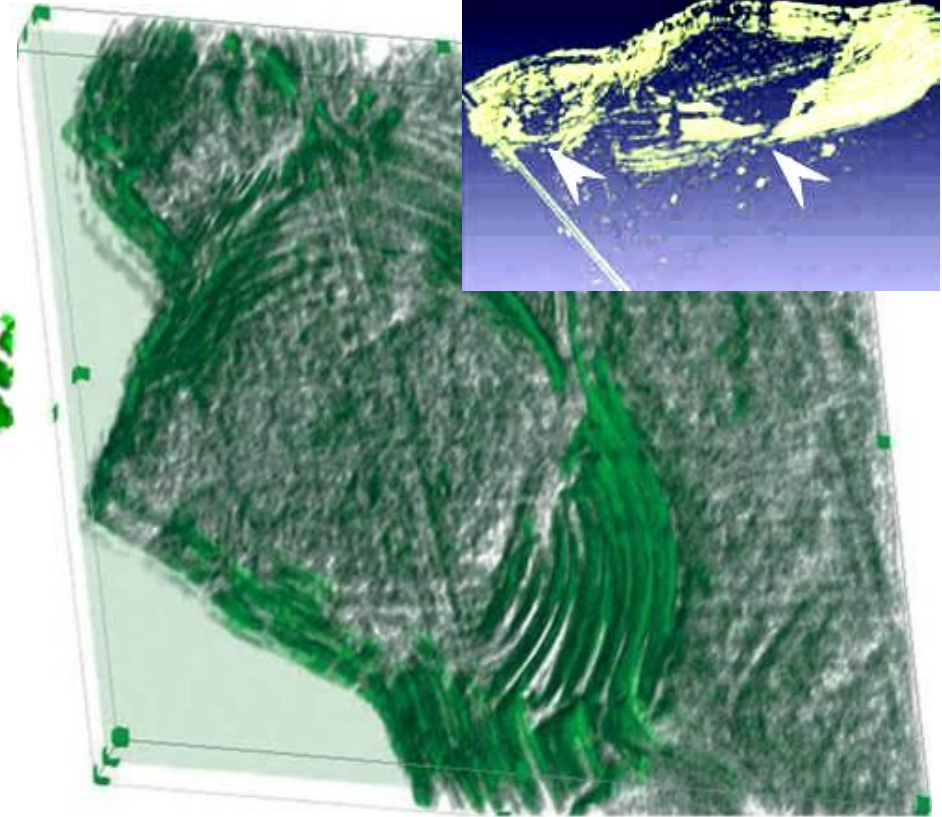
A. Alekseev et al, *Adv. Func. Mater.*, 2012, 22, 1311.



Study of biological objects and materials

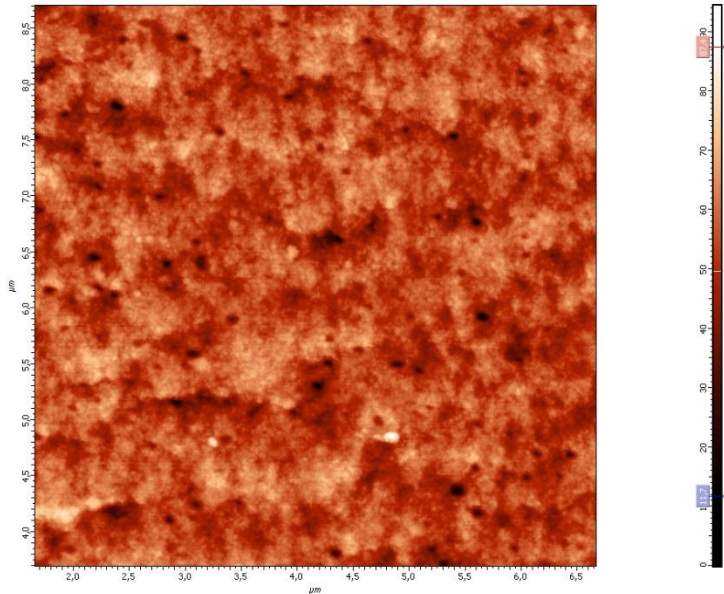
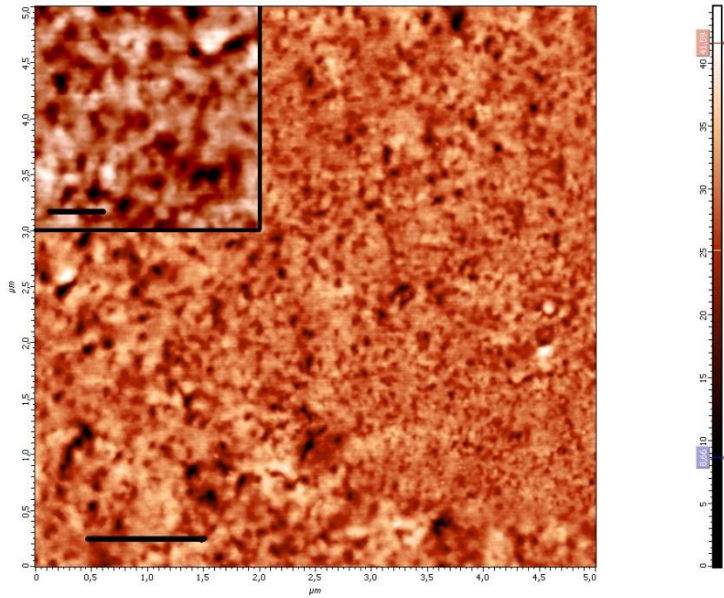


3D reconstruction: porous biodegradable cell matrix made by electrospinning of polyoxybutirate and used for regenerative medicine. 20 sections, 41.2 34.1 8.5 μm

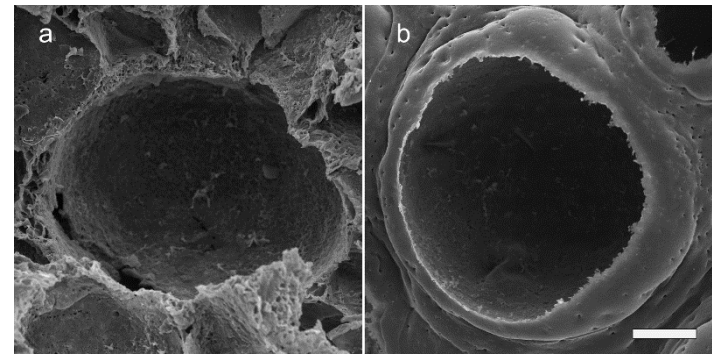


3D-reconstruction of antenna sensillas of the wasp, 12.5 13.0 0.7 μm , 11 sections, 70 nm section thickness.

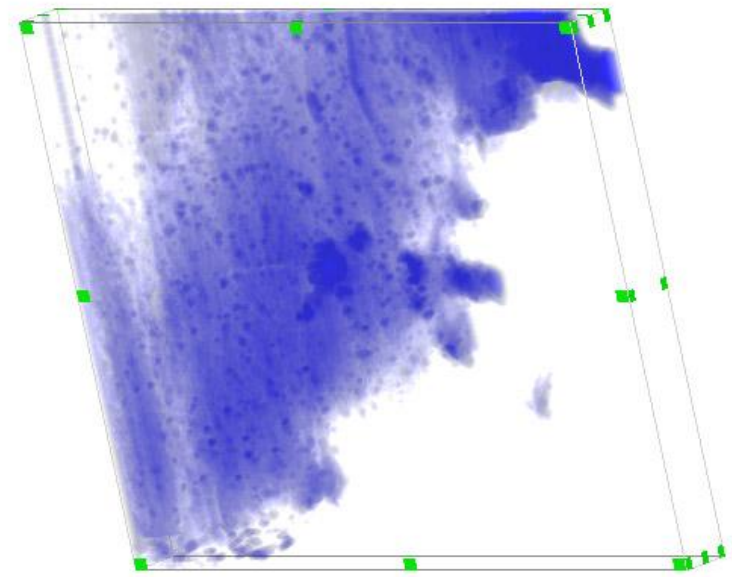
A. E. Efimov, H. Gnaegi, R. Schaller, W. Grogger, F. Hofer and N. B. Matsko, Soft Matter, 2012, DOI:10.1039/c2sm26050f



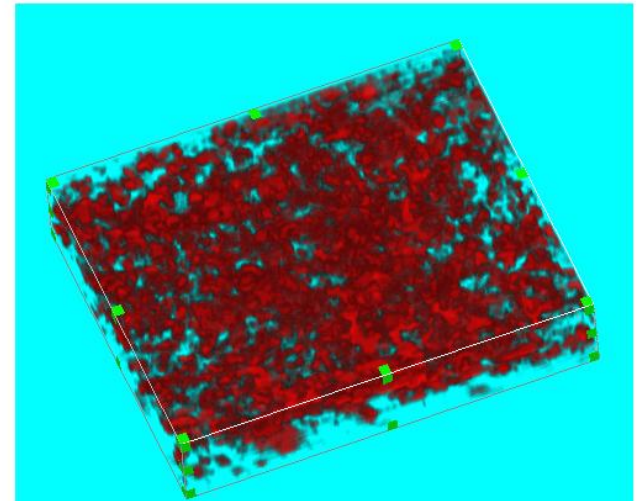
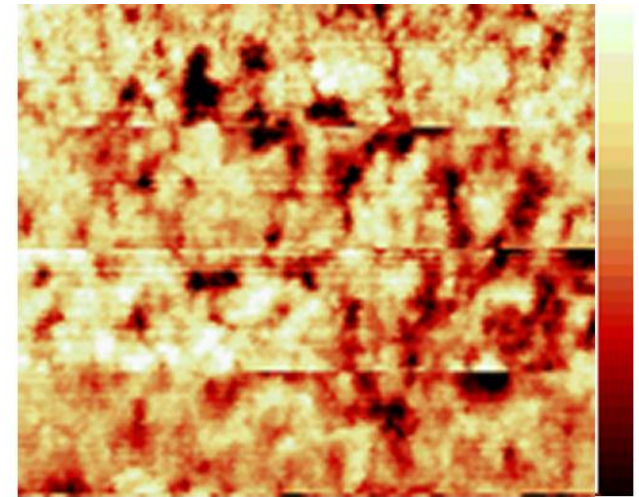
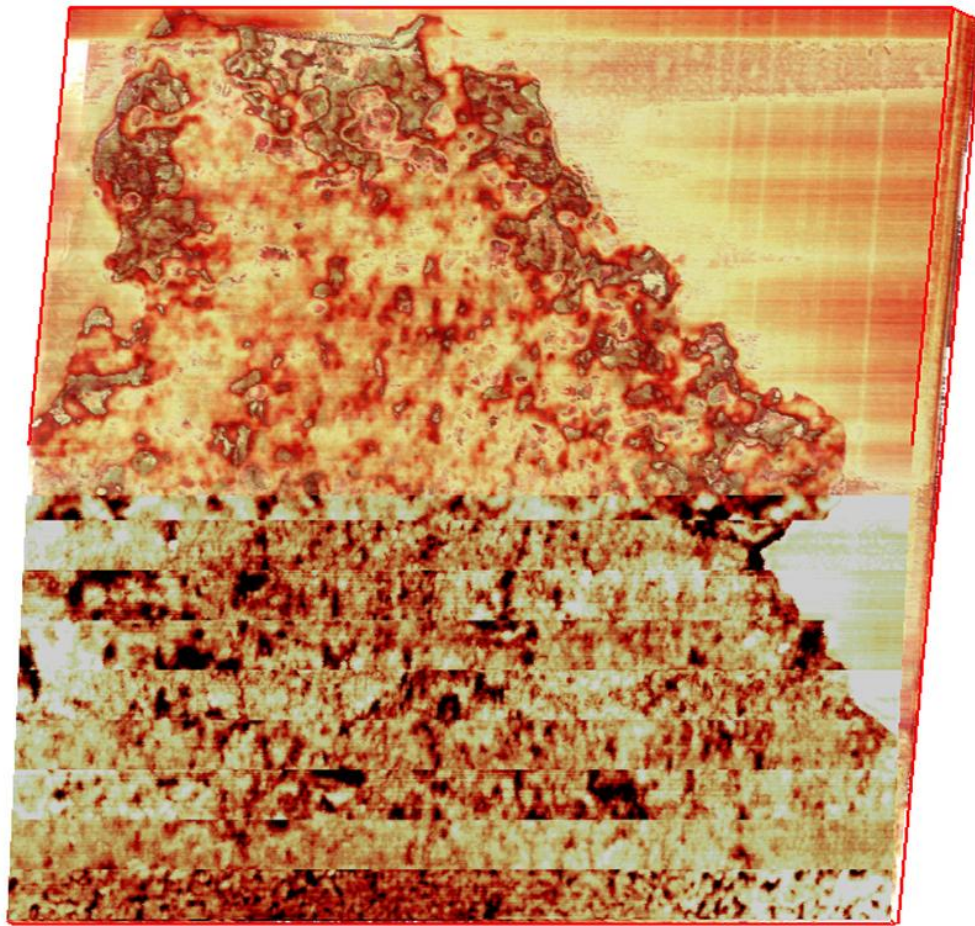
AFM images of block face surface of spidroin (a) and fibroin (b) scaffolds after ultramicrotome sectioning, 5x5 μm. Scale bar - 1 μm, scale bar in insert (a) - 200 nm.



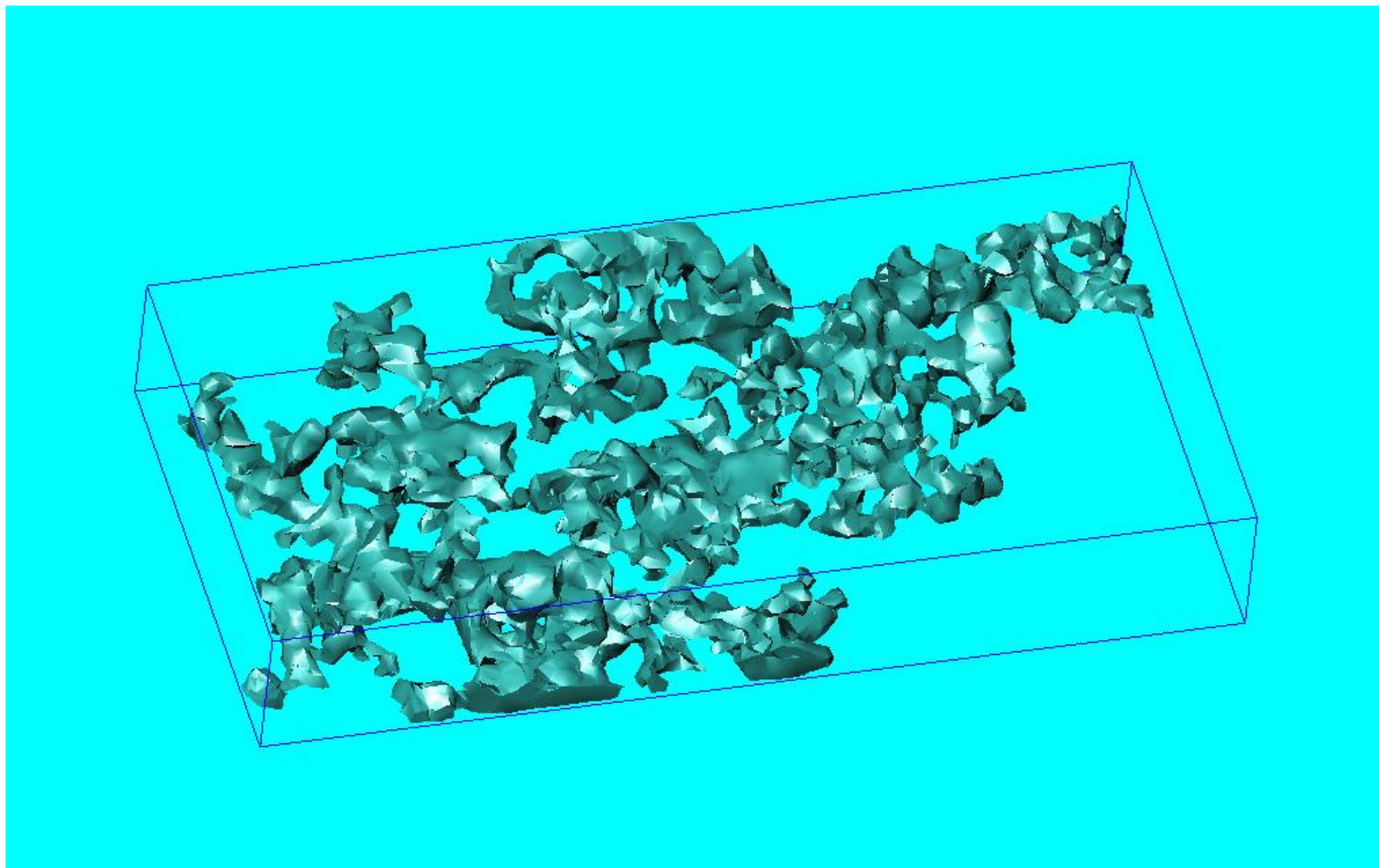
SEM images of rS1/9 (a) and fibroin (b) scaffold macropores. Scale bar 100 μm



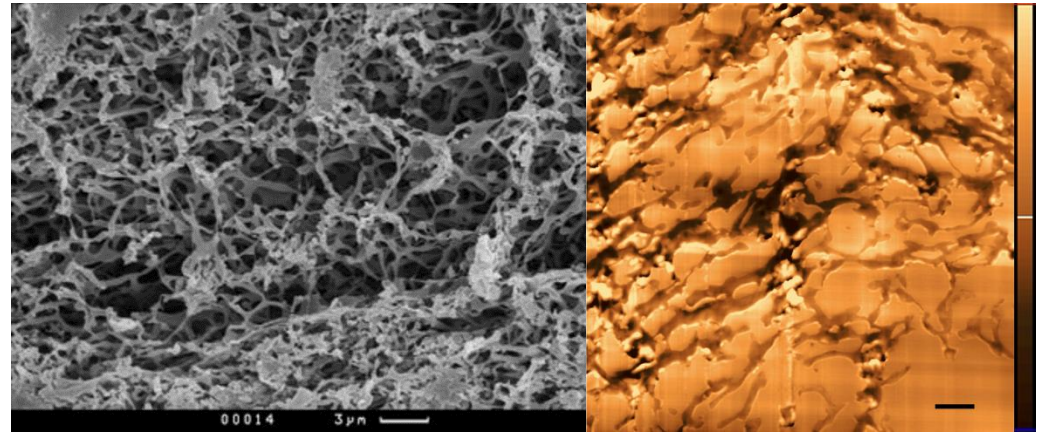
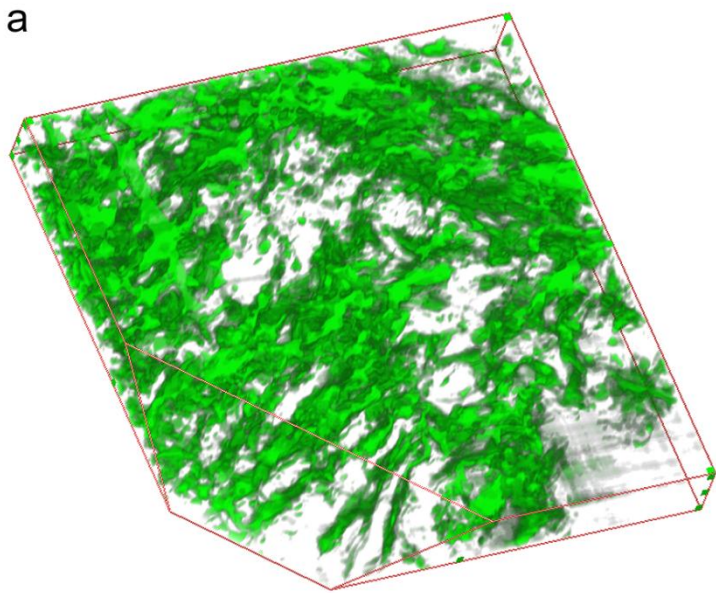
3D-reconstruction of fibroin-based scaffold (12 sections, 45.5 32.8 1.8 μm), porosity = 0.5%



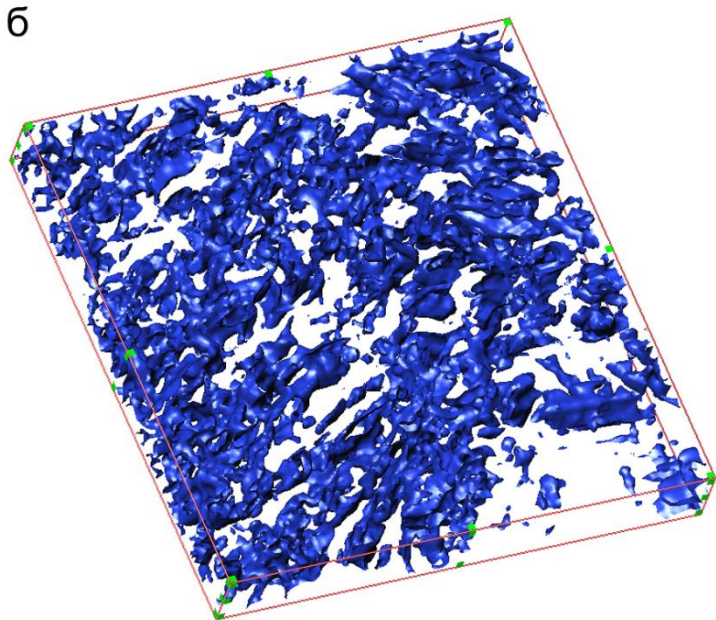
SPNT 3D-reconstruction of spidroin scaffold macropore wall, overview, 15.0x15.0x1.0 μm ; (b) close-up of inclined section of 3D-reconstruction volume, height variation; (c) SPNT 3D-reconstruction of pore volume in spidroin scaffold, 4.68x4.0x0.9 μm , porosity = 24%



Cluster of interconnected nanopores in spidroin scaffold;
Porosity 24% > 3D percolation porosity threshold (16% universal value)
Interconnected pore volume = 8.4% of total volume or 35% of total pore volume

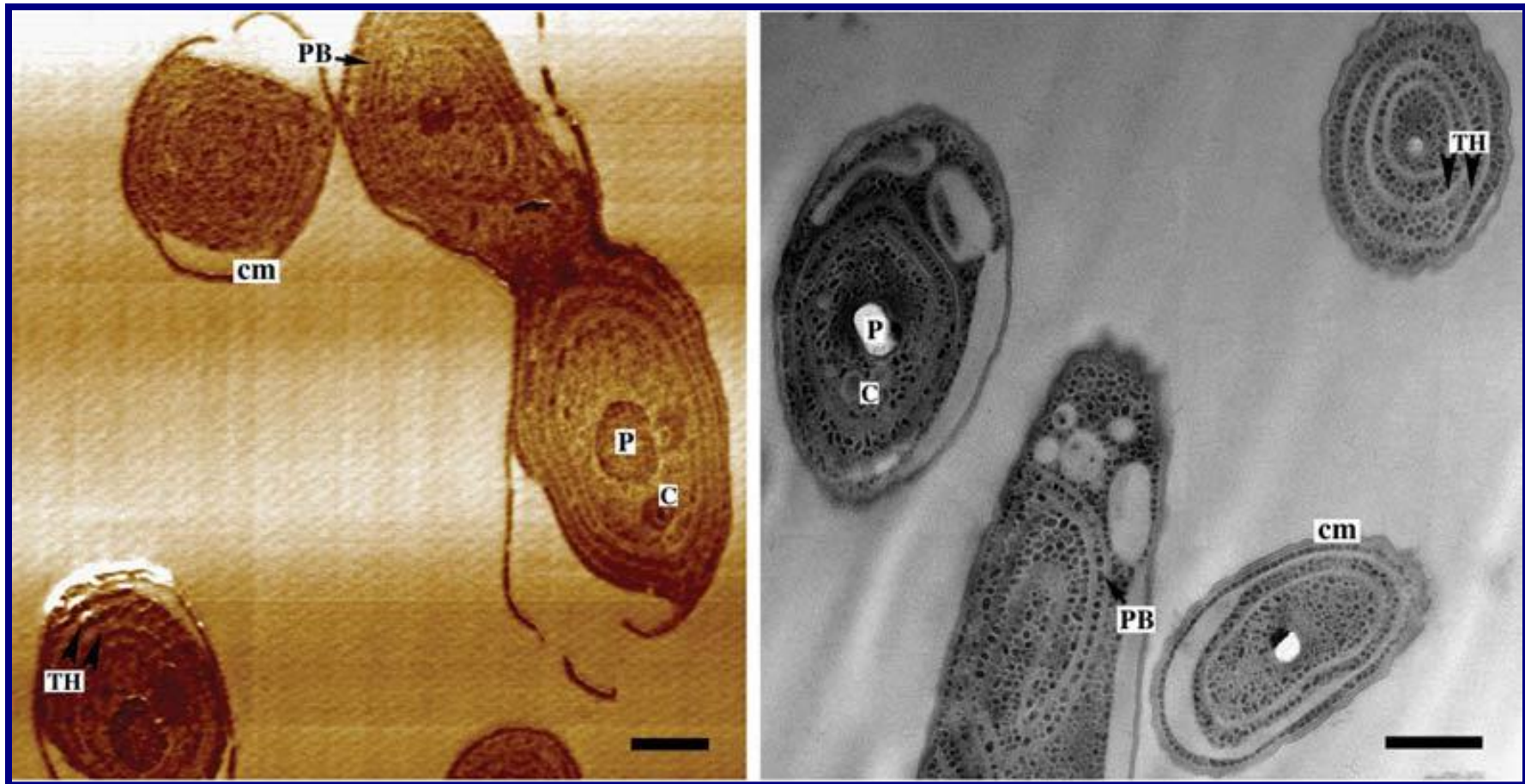


SEM image of fibroin scaffold,
SPM image of surface of fibroin scaffold
section. (image size 33.0 33.0 μm)



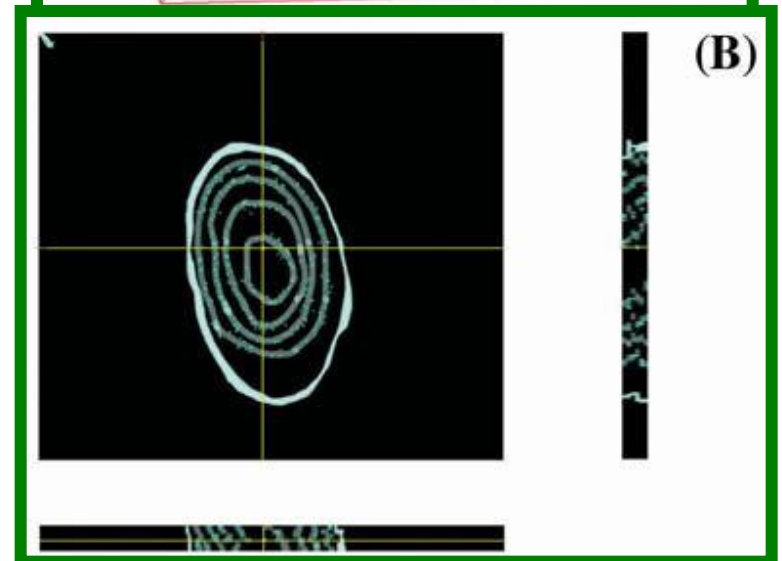
Three-dimensional reconstruction of fibroin
scaffold structure (a) and reconstruction of
the volume of interconnected micropores
(b) in the same volume,
26.7 28.1 4.2 μm, porosity = 65,7%

АСМ/ПЭМ (изображения структуры цианобактерии *Synechococcus*)



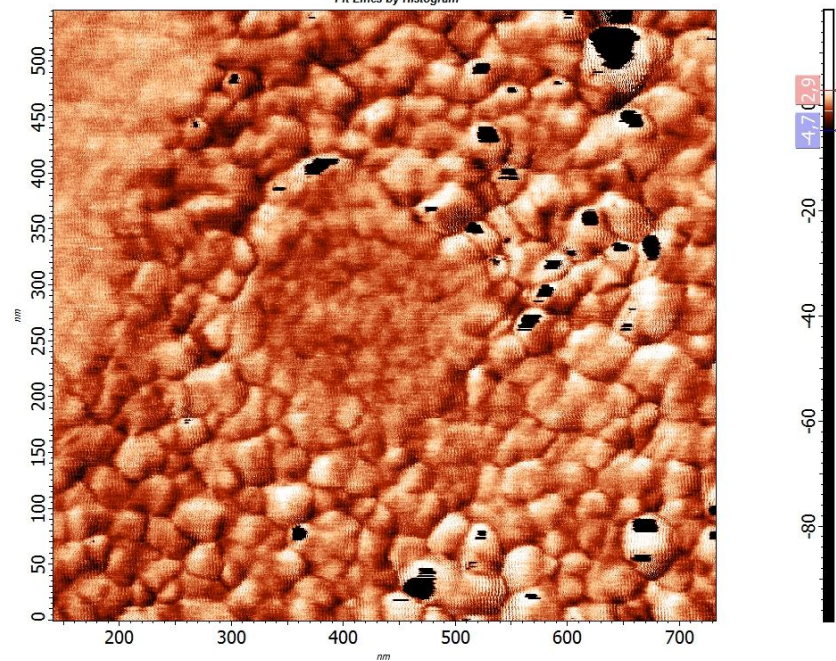
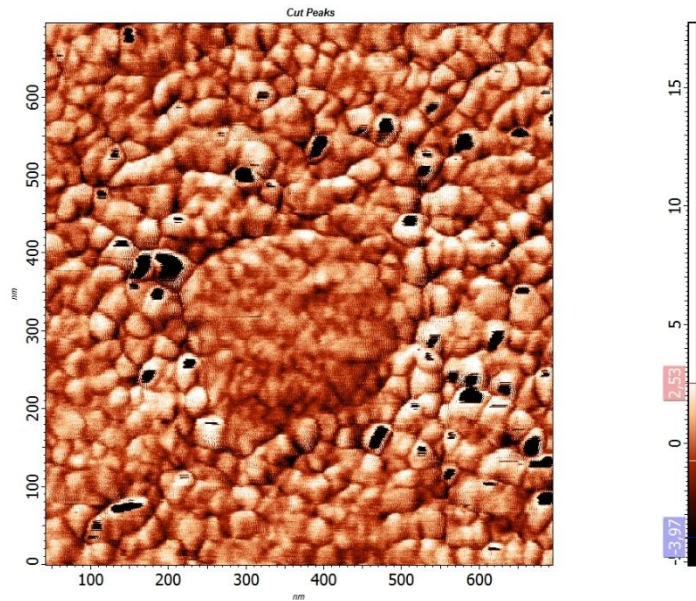
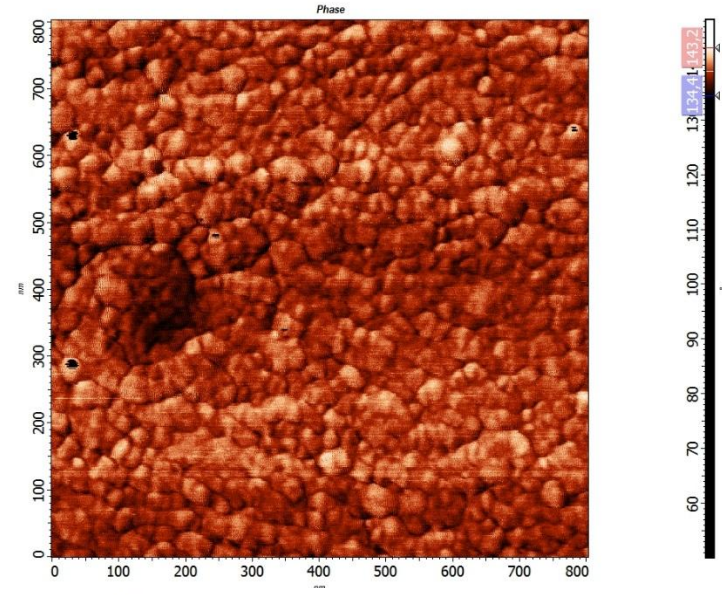
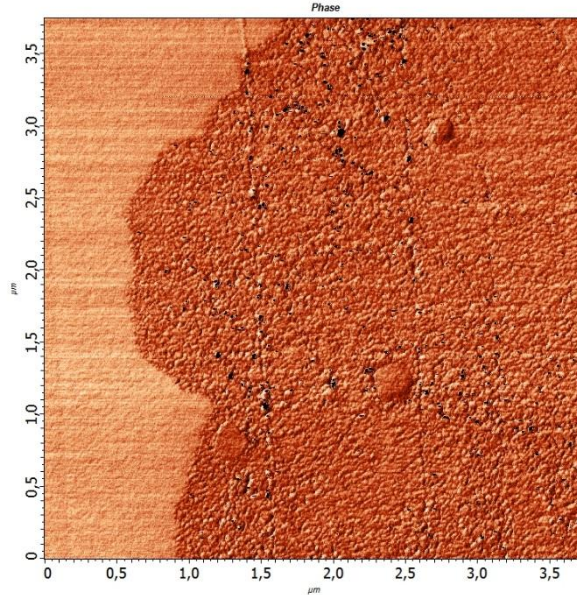
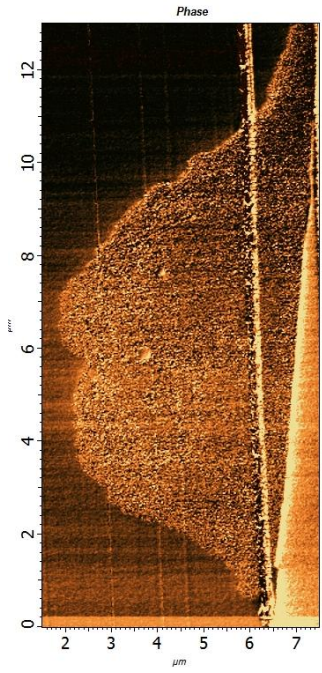
Размерный отрезок 500 нм., cm – клеточная мембрана, TH -тилакоид, PB - фикобилисомы, P полифосфатная гранула, C- карбоксисома.

AFM 3D reconstruction of cyanobacteria *Synechococcus* membrane structure



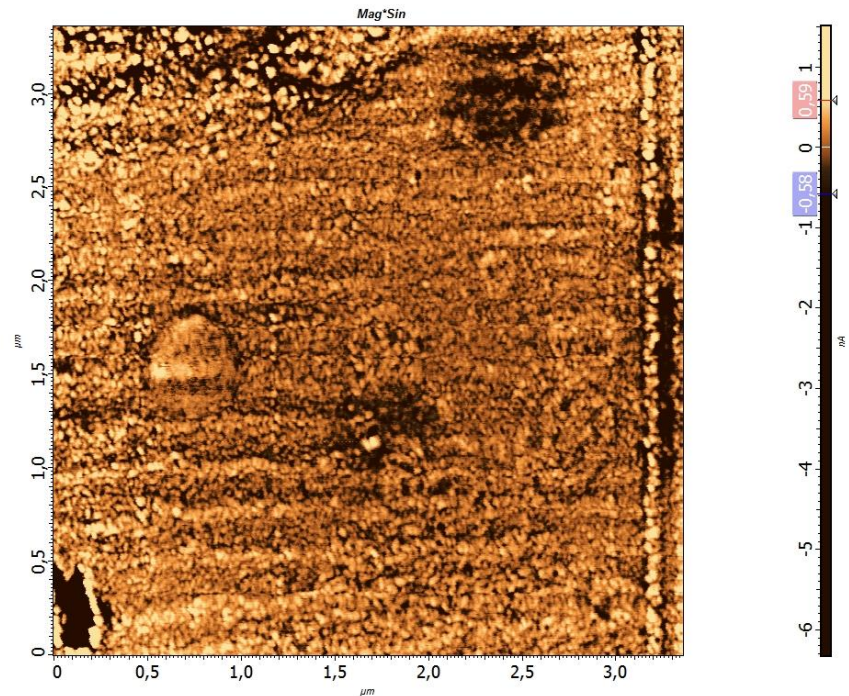
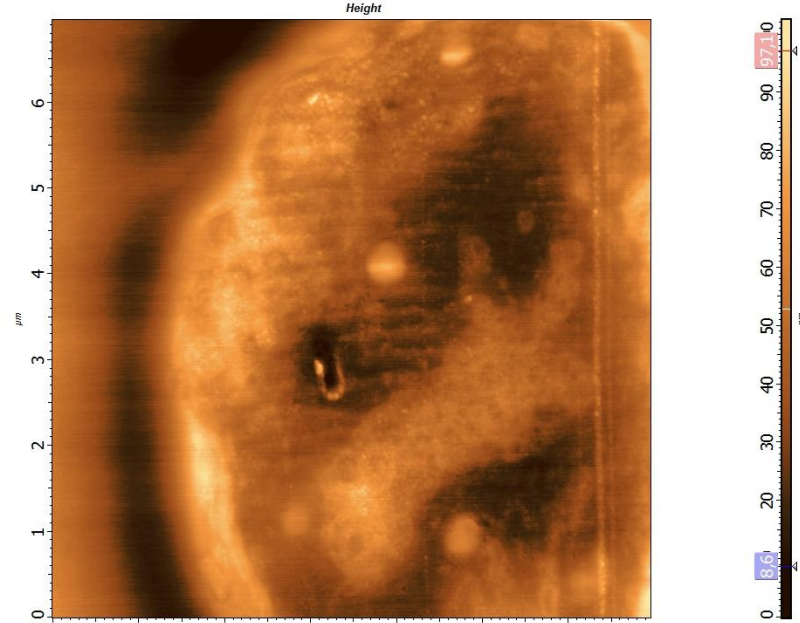
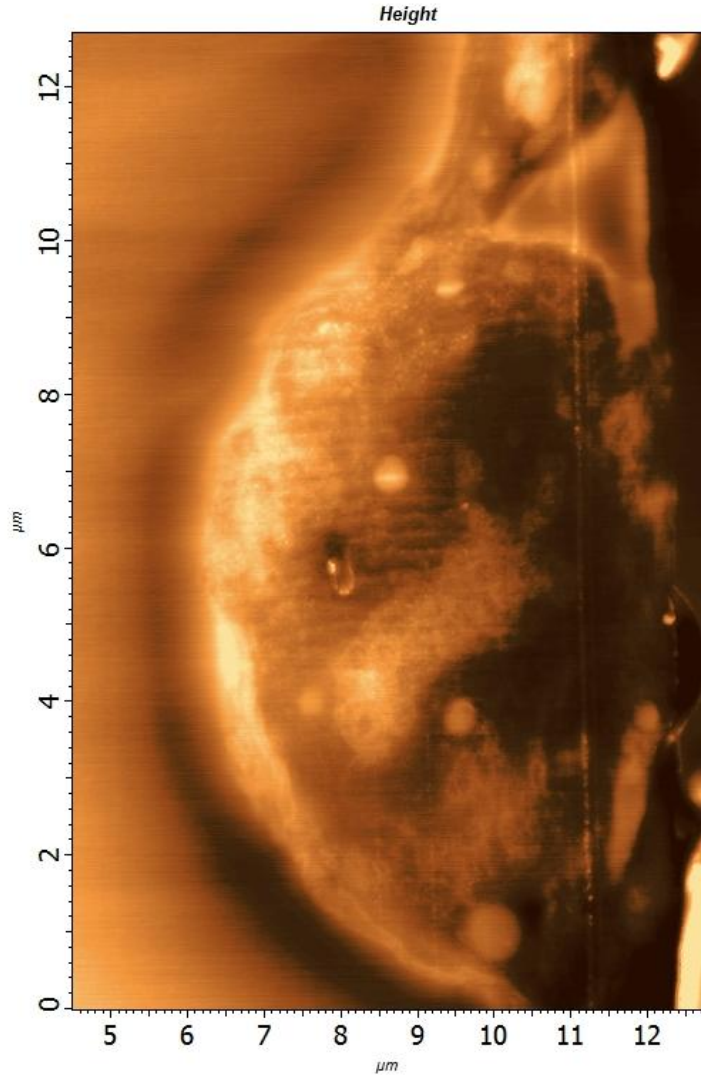
Resulted volume image contains $432 \times 398 \times 6$ voxels what corresponds to physical size of $2.7 \times 2.5 \times 0.15 \mu\text{m}$.

AFM of cardiomyocytes



Samples courtesy of K.I. Agladze group, MIPT

AFM of cardiomyocytes (surface treated by ethanol)



Samples courtesy of K.I. Agladze group, MIPT

Ethanol treatment described in
N.B.Matsko, *Ultramicroscopy*. 2007; 107: 95–105

Different sample preparation techniques

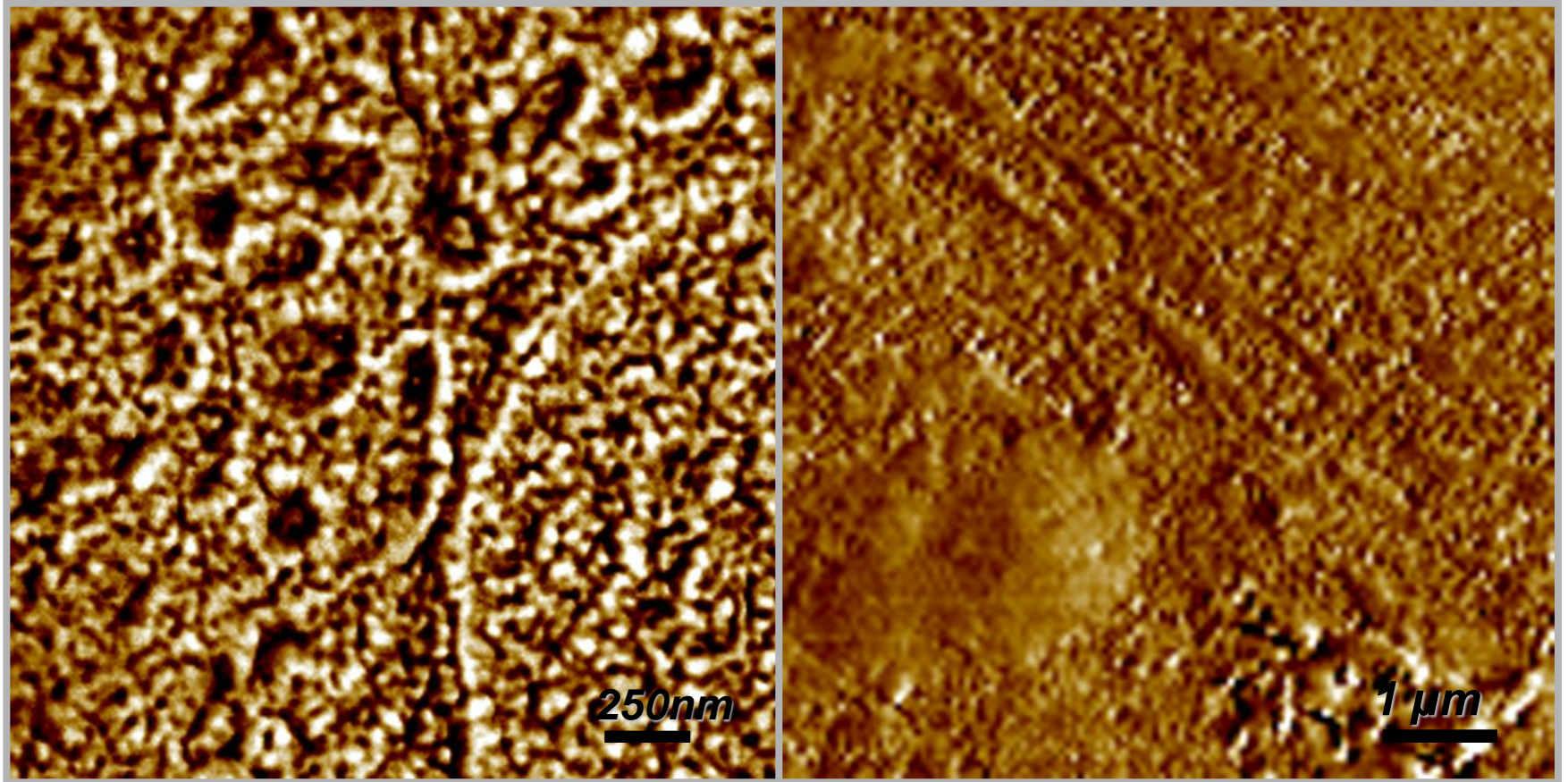


*Cryo fixation
Freeze
substitution*



*Chemical fixation
Rapid dehydration*

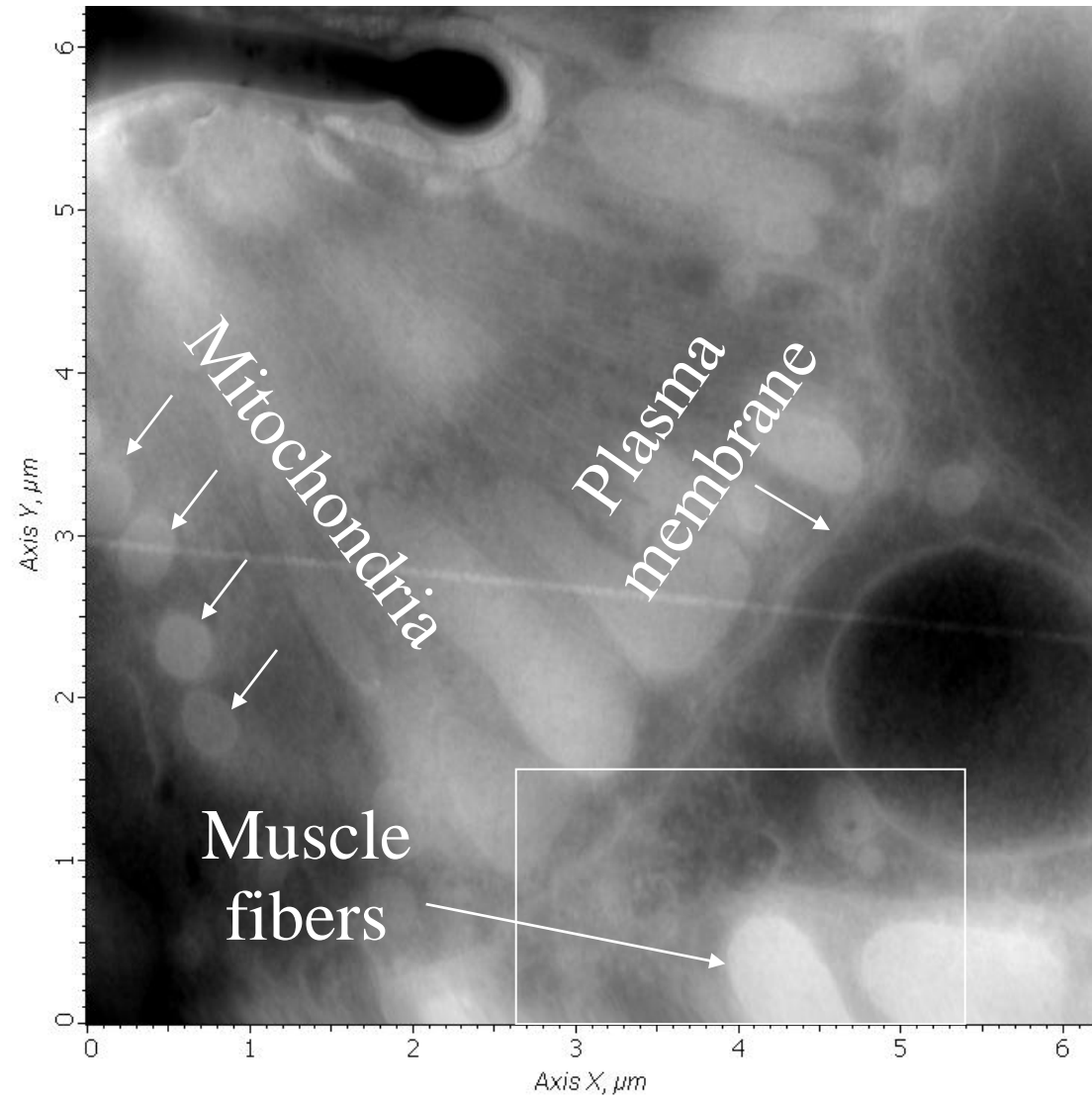
Sample preparation



Cryofixation (high-pressure freezing)

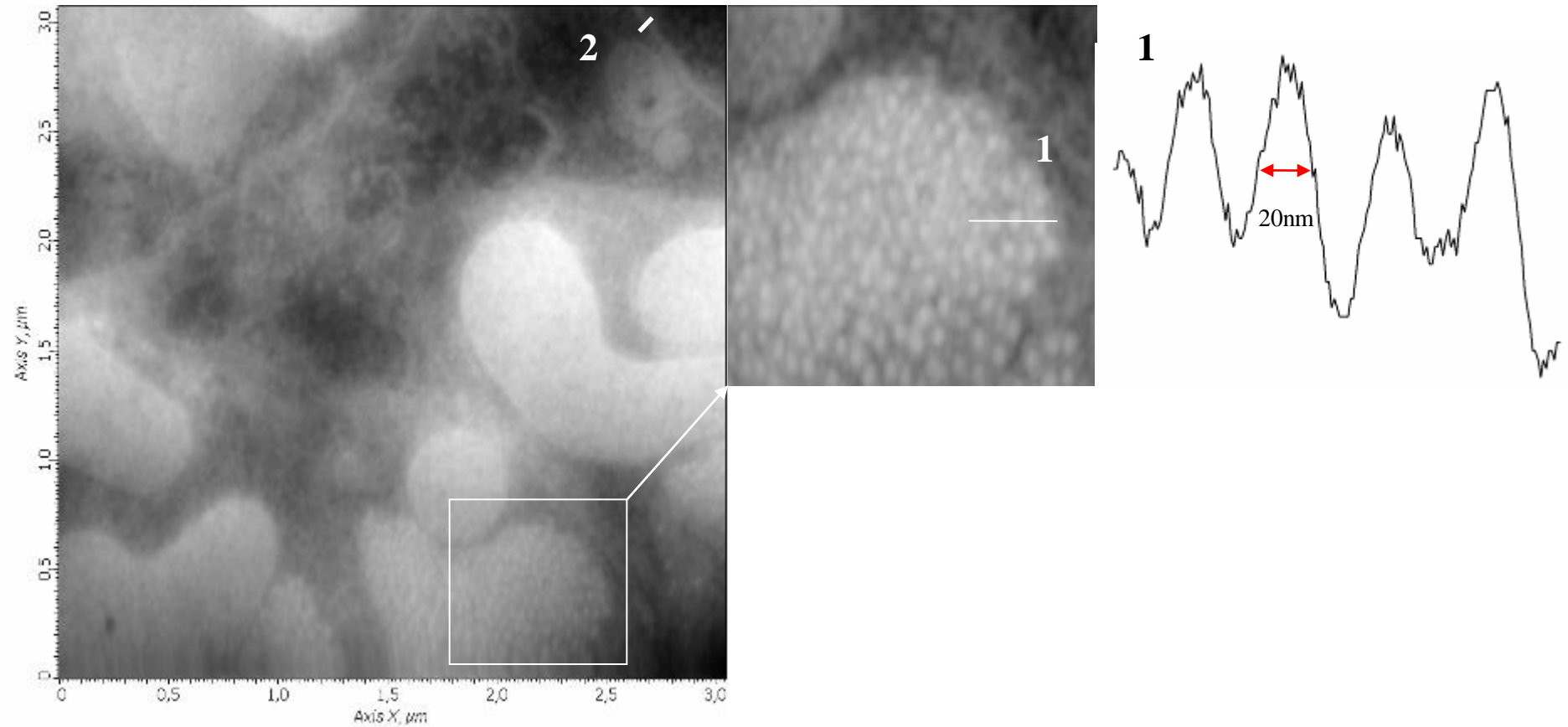
Chemical fixation

Cell morphology



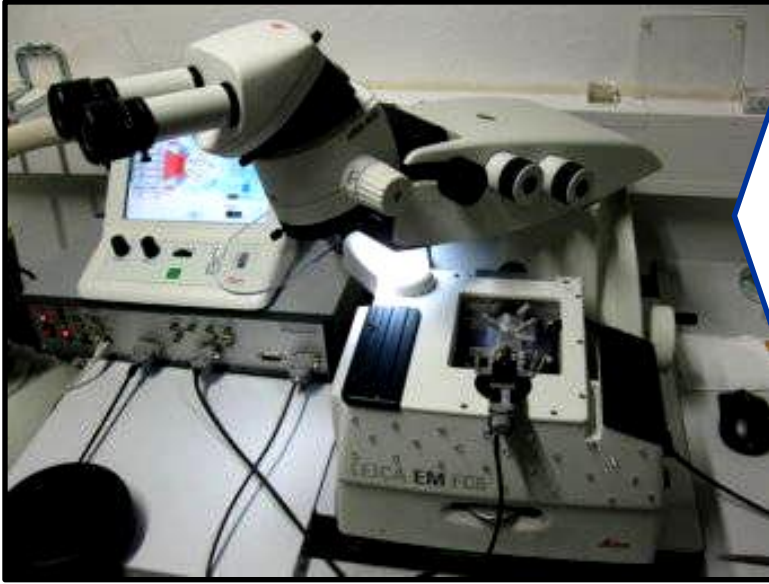
Fragment of nematode *C. elegans*..

Nanomorphology of cell structures

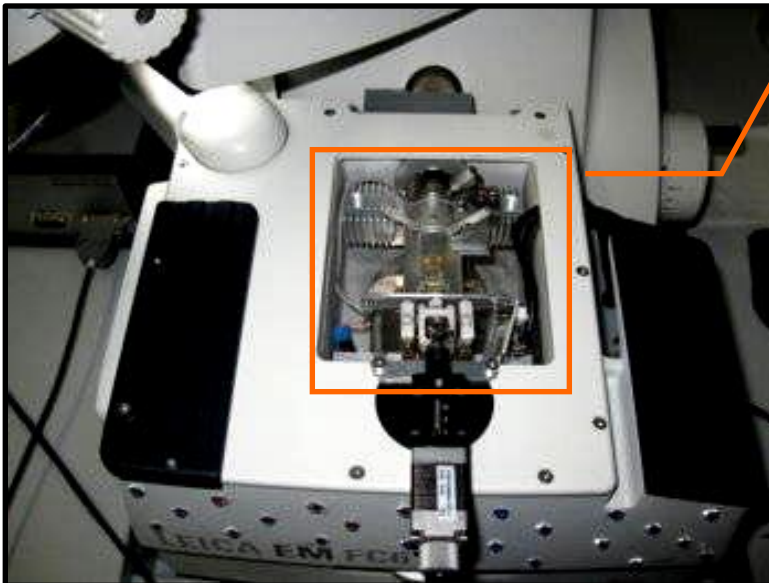


Fragment of nematode *C. elegans*. Muscle fibers.

2. Cryoultramicrotome + AFM (for *in-situ* soft matter study)



Leica EM UC6/FC6 cryoultramicrotome performs ultrathin sectioning of soft materials at temperatures from -15 to -190 C. Section thickness ranges from 20 nm to 1 μ m.

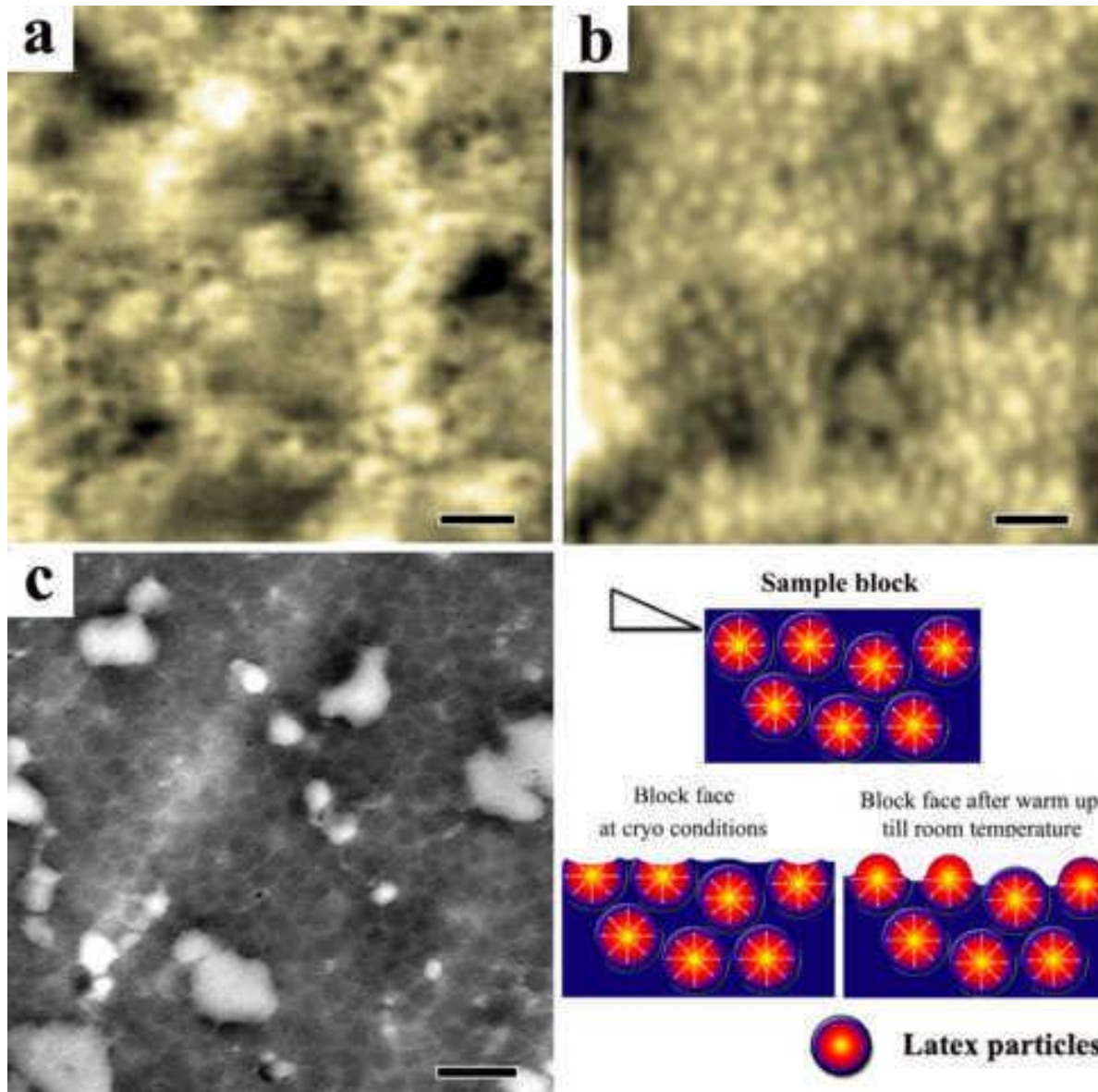


Cryo-AFM measuring head is installed directly into the cryochamber of the ultramicrotome



Tuning fork-based AFM probe

CryoUMT/AFM application results



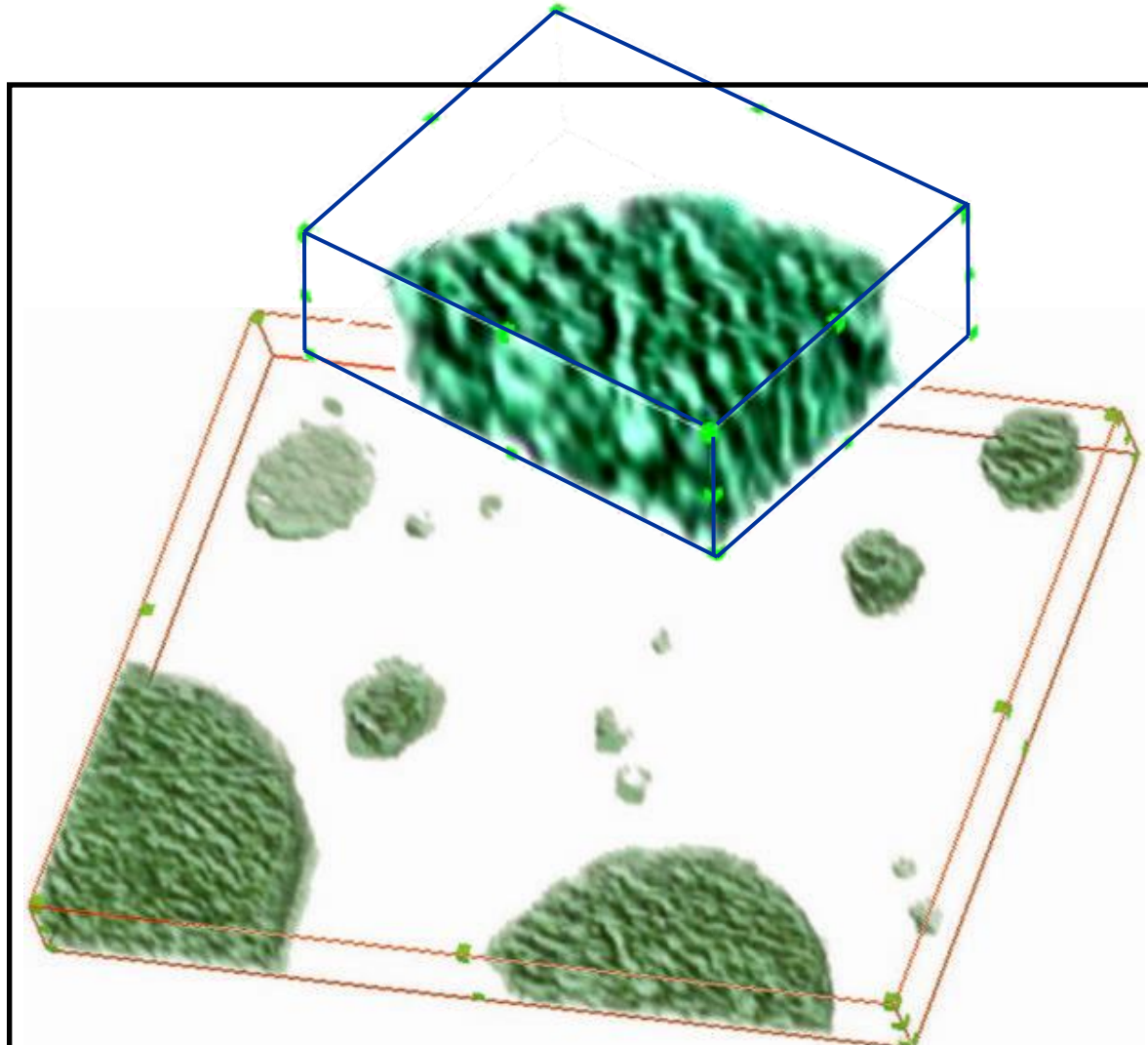
The morphology of a cross-section of a nitrile butadiene-rubber latex sample characterized by cryo-AFM and TEM.

(a) A topographical AFM image of an epoxy embedded latex stripe that was mounted in the cryo-chamber of SNOTRA, cryo-sectioned and immediately scanned at -120 C.

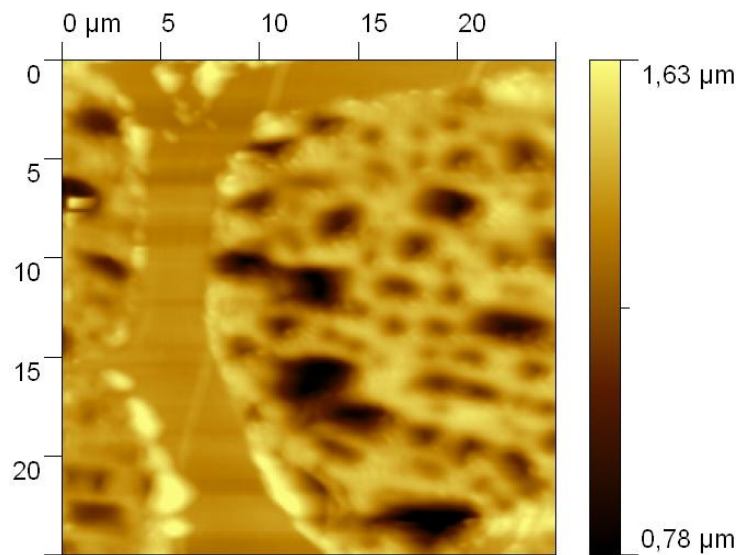
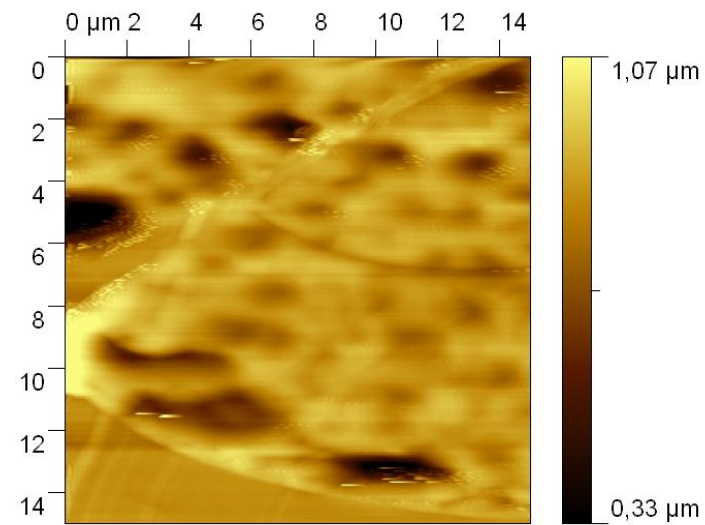
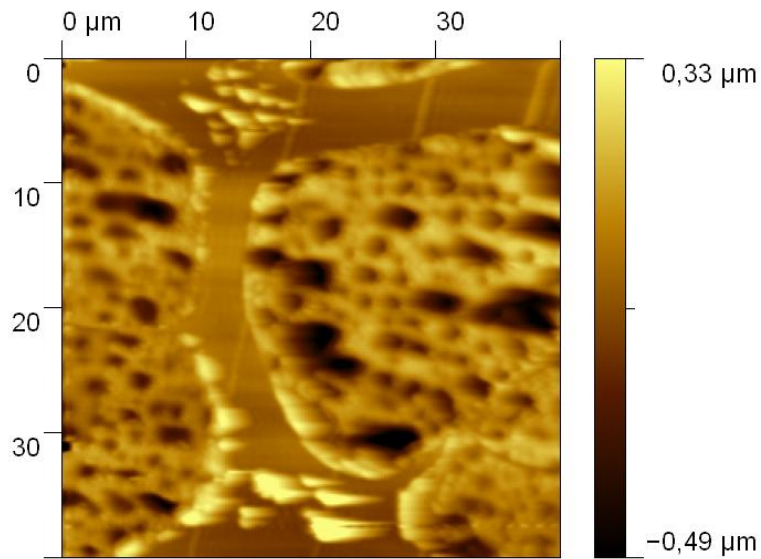
(b) Immediately afterwards, the same sample was warmed to room temperature and then examined using the same AFM
(c) A TEM image of the last thin section of the NBR latex sample.
(d) A schematic description of the topographical change of the sample block phase that took place during sectioning and the following warming processes. The scale bars in (a, b, c) are 200 nm, and the topographical variations in (a) was 27.2 nm, and in (b) was 35.5 nm.

3D study of soft polymers and composites with cryoUMT/AFM

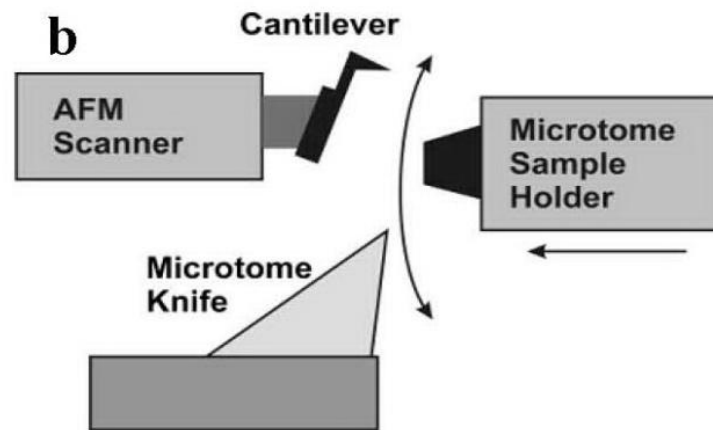
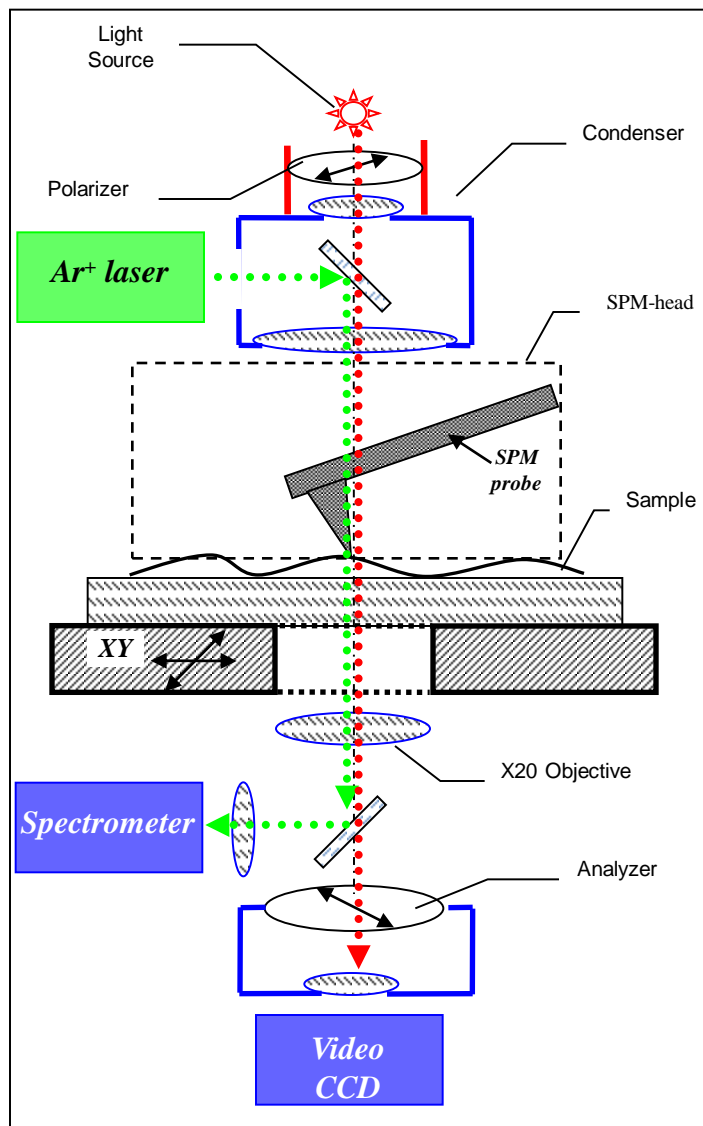
3D reconstruction of polymer composite PA6/SAN at -80 C: 6 sections of 125 nm, 7.9 6.2 0.75 μm and 2.0 2.0 0.75 μm , correspondingly.



Spherogel analysis by cryoSPM after section at -80 C

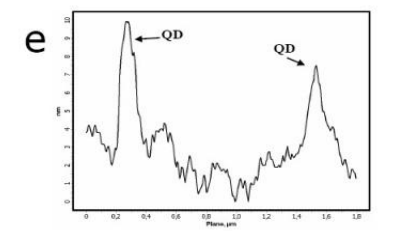
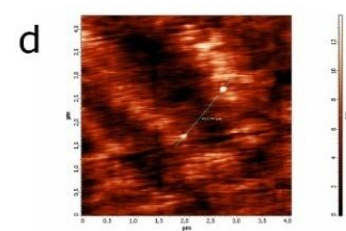
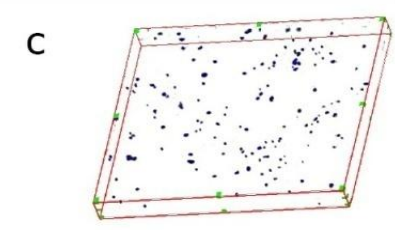
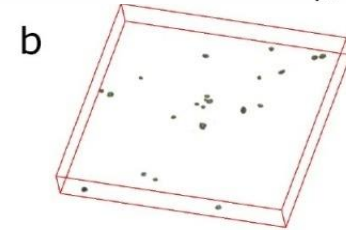
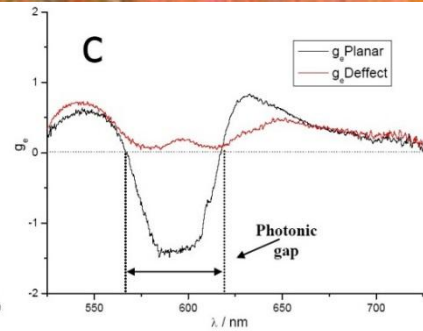
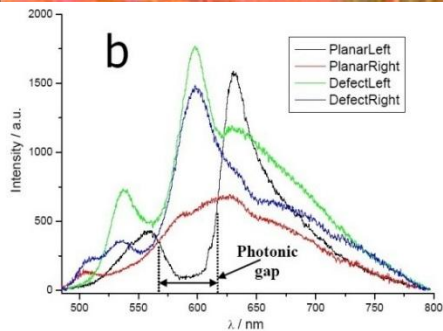
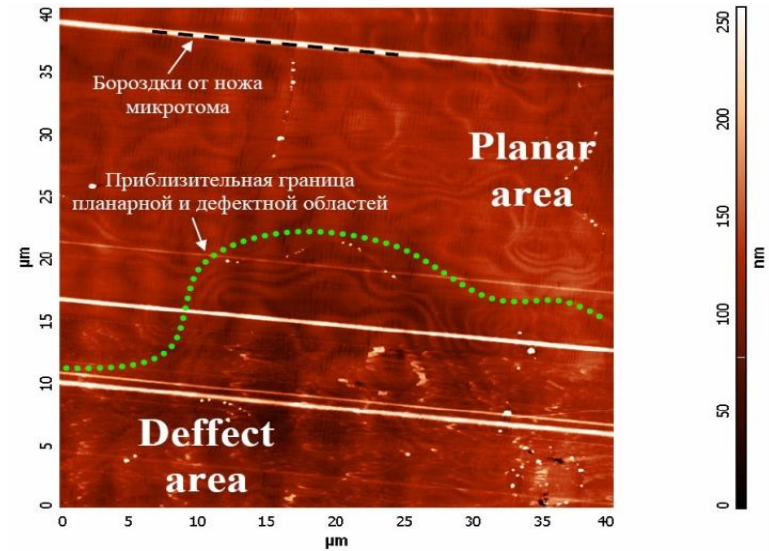
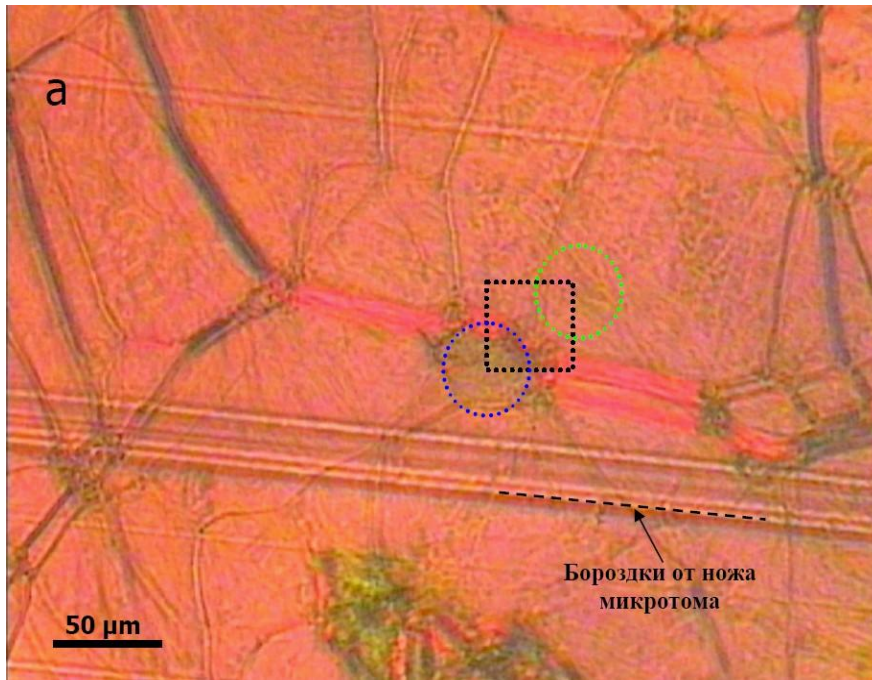


3. Correlative 3D-AFM/UMT and AFM/POM (polarized optical microscopy) measurements



Measurements are performed on the same sample area but sample transfer is still needed between AFM/POM and AFM/UMT combined systems

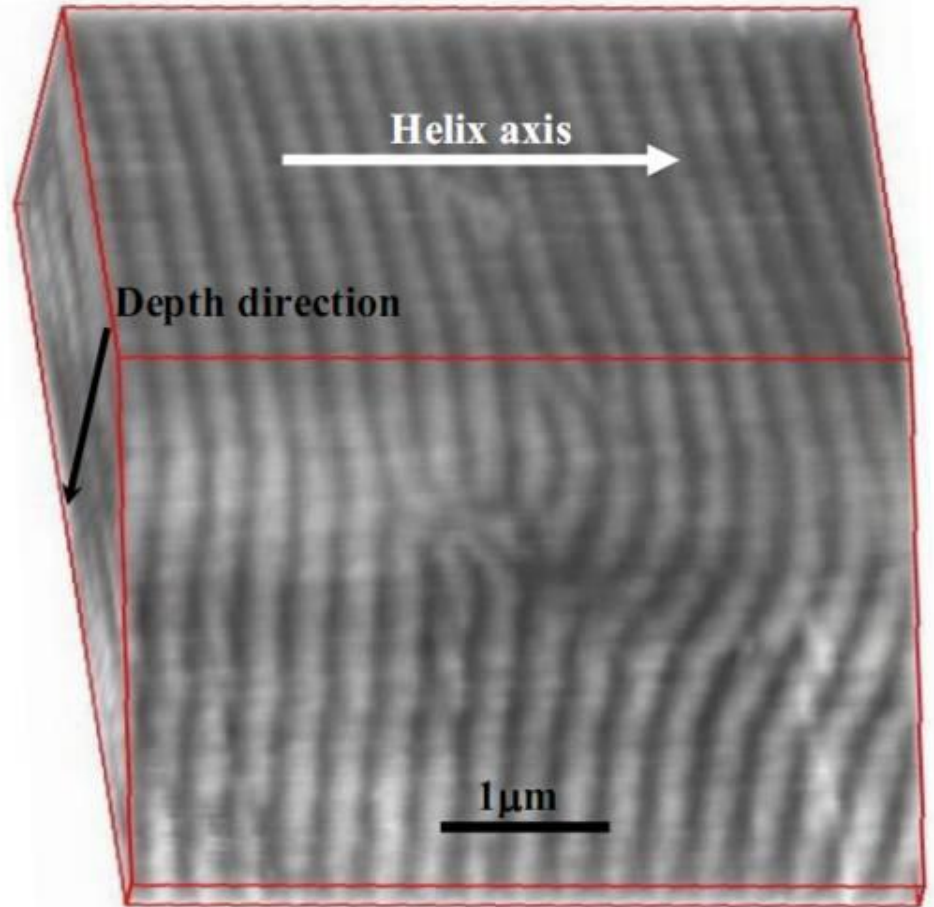
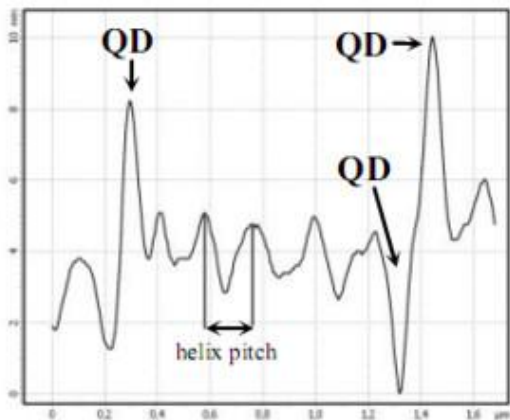
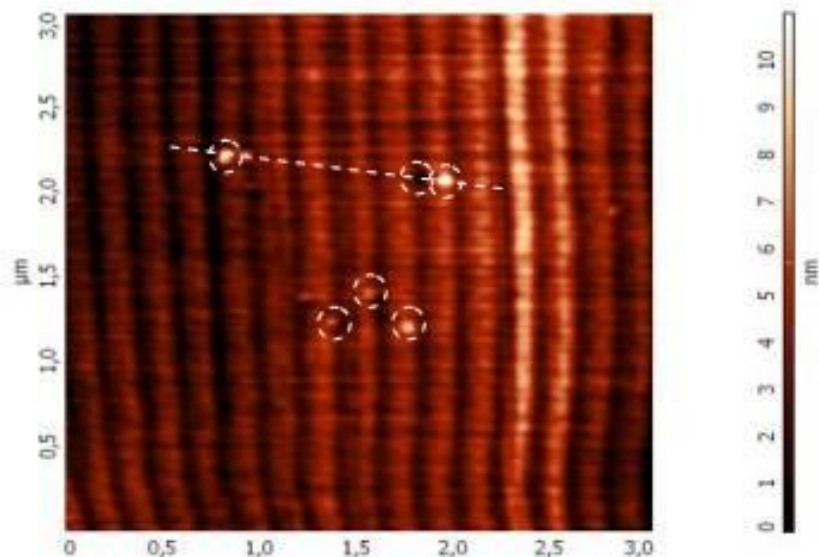
AFM, 3D-AFM and fluorescence POM correlative analysis of LC/QD nanocomposite



a) POM-image of the microtomed LC sample surface, green circle – planar area, blue circle – defect area, square marks AFM image area b) Left- and right – circular polarized components of implanted QD fluorescence. c) dissymmetry factor of QD fluorescence in planar and defect zones $g_e = 2 (IL - IR) / (IL + IR)$

a) AFM image of area including planar and defect zones. b) 3D-AFM reconstruction of QD distribution in the planar zone, 5X5X0,7 μm c) 3D-AFM reconstruction of QD clusters distribution in the defect zone, 50X50X5 μm. d) AFM image of planar zone with individual QD e) Cross-section profile of image 2d.

3D study of liquid crystal / quantum dots nanocomposite

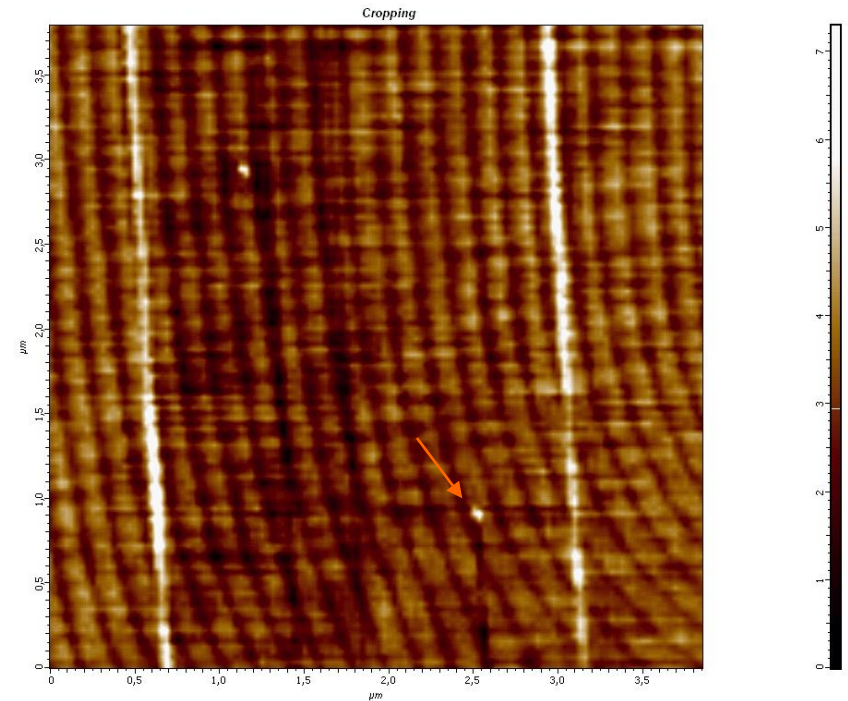
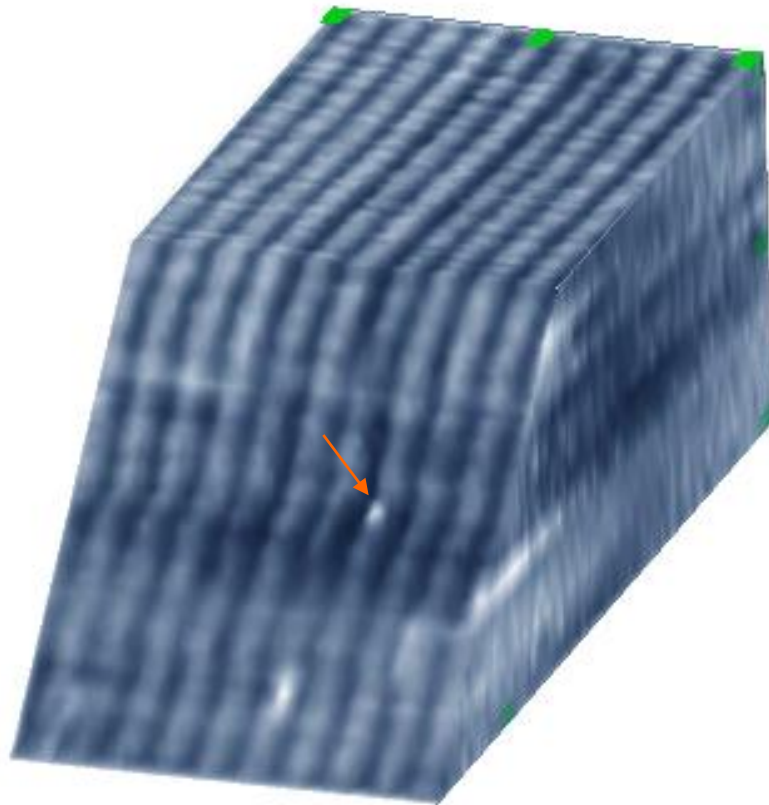


AFM image and 3D-reconstruction of cholesteric liquid crystal structure with implanted fluorescent CdSe/ZnS quantum dots, 14 sections, 100 nm section thickness

Mochalov KE, Efimov AE, Bobrovsky A, Agapov II et al, ACS Nano. 2013; 7 (10): 8953–8962.

Mochalov KE, Efimov AE, Bobrovsky A, Agapov II et al, Proc. SPIE 8475, Liquid Crystals XVI, 847514, 2012.

3D study of liquid crystal / quantum dots nanocomposite



3D-AFM reconstruction and 2D AFM image (4x4 μm) of cholesteric LC structure with implanted fluorescent CdSe/ZnS quantum dots, 14 sections, 100 nm section thickness. (arrows indicate the same QD on AFM image and 3D AFM reconstruction).

We observe that implanted QD do not distort the planar LC structure

4. Project for perspective development: Combination of ultramicrotomy and SPM with light microscopy and microspectroscopy (nanoRaman) *in situ*

Applications:

- Nanocomposites
- Liquid crystals
- Soft polymer composites
- Biological objects and materials
- Semiconductors

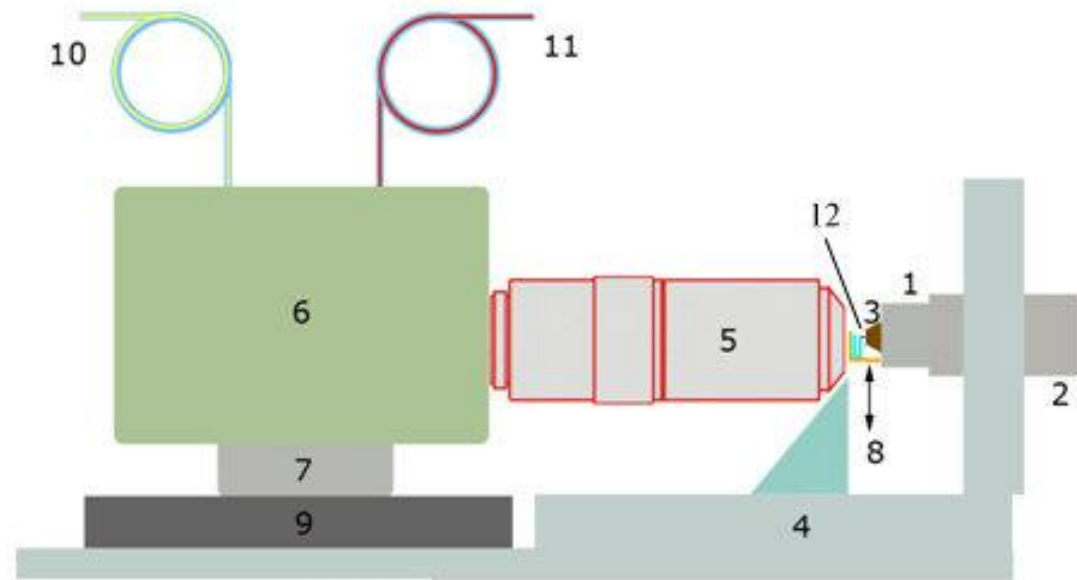
Study of:

Local chemical structure (also with TERS-improved resolution);

Local optical and fluorescence properties;

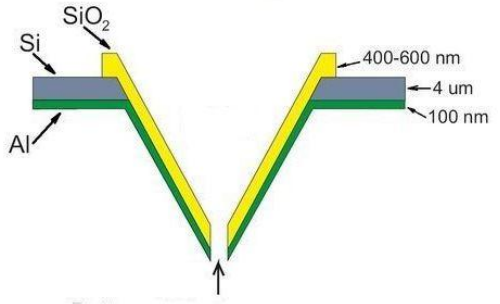
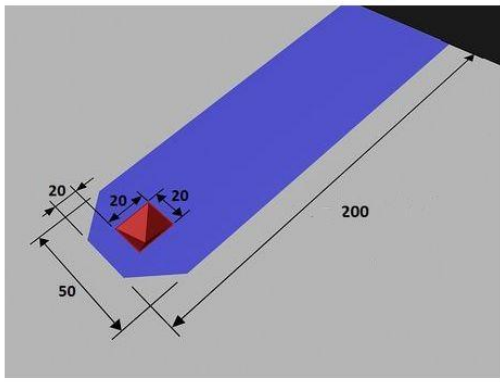
3D Raman and AFM imaging at temperatures from -120 C to 50 C;

3D-Raman imaging of non-transparent samples in the bulk

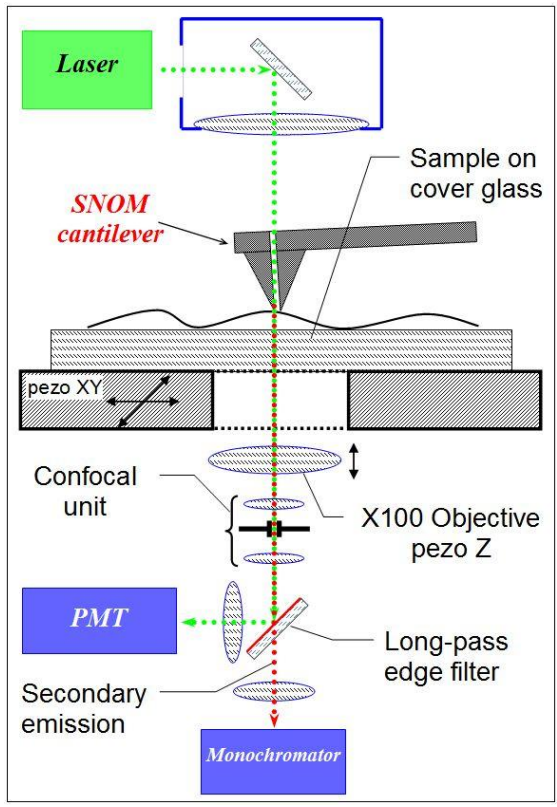
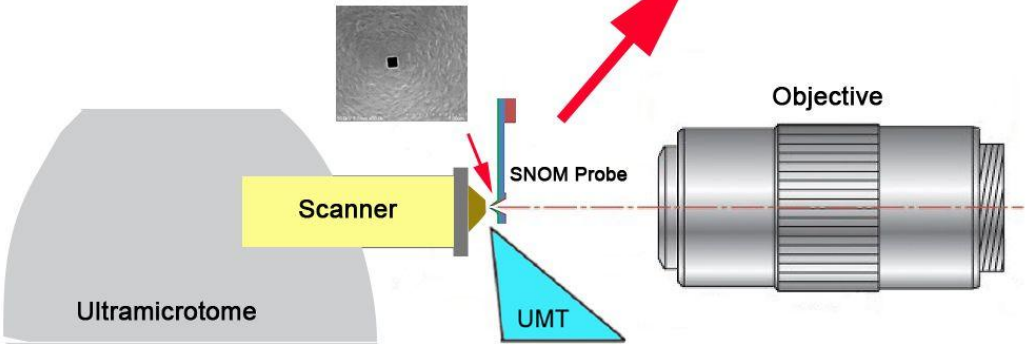
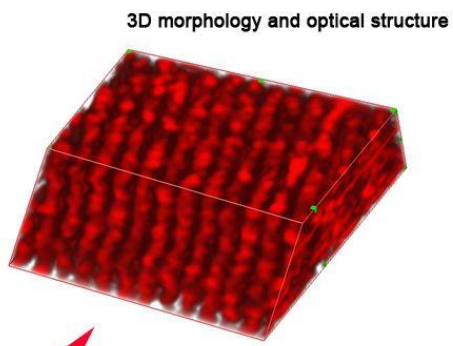
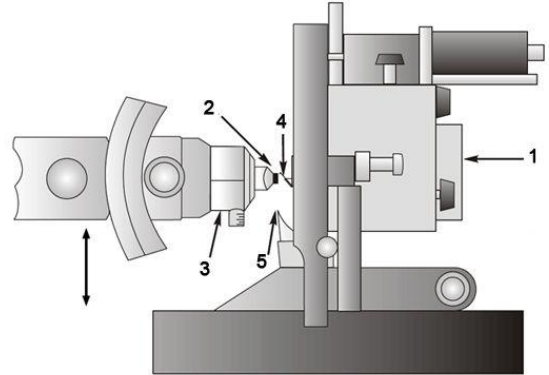


- 1 – sample holder with a piezotube XYZ scanner,
- 2 – movable ultramicrotome arm, 3 – sectioned sample,
- 4 – cryochamber,
- 5 – high-aperture optical objective, 6 – optical module,
- 7 – precise objective micropositioner,
- 8 – diamond knife, 9 – optical module platform,
- 10 – optical fiber for the laser excitation light,
- 11 – optical fiber guide to the spectrometer monochromator for the spectral analysis.
- 12 – tuning fork-based AFM tip

What is SNONT? Scanning nearfield optical nanotomography (SNONT) is the combination of confocal optical microspectroscopy, SNOM and SPNT

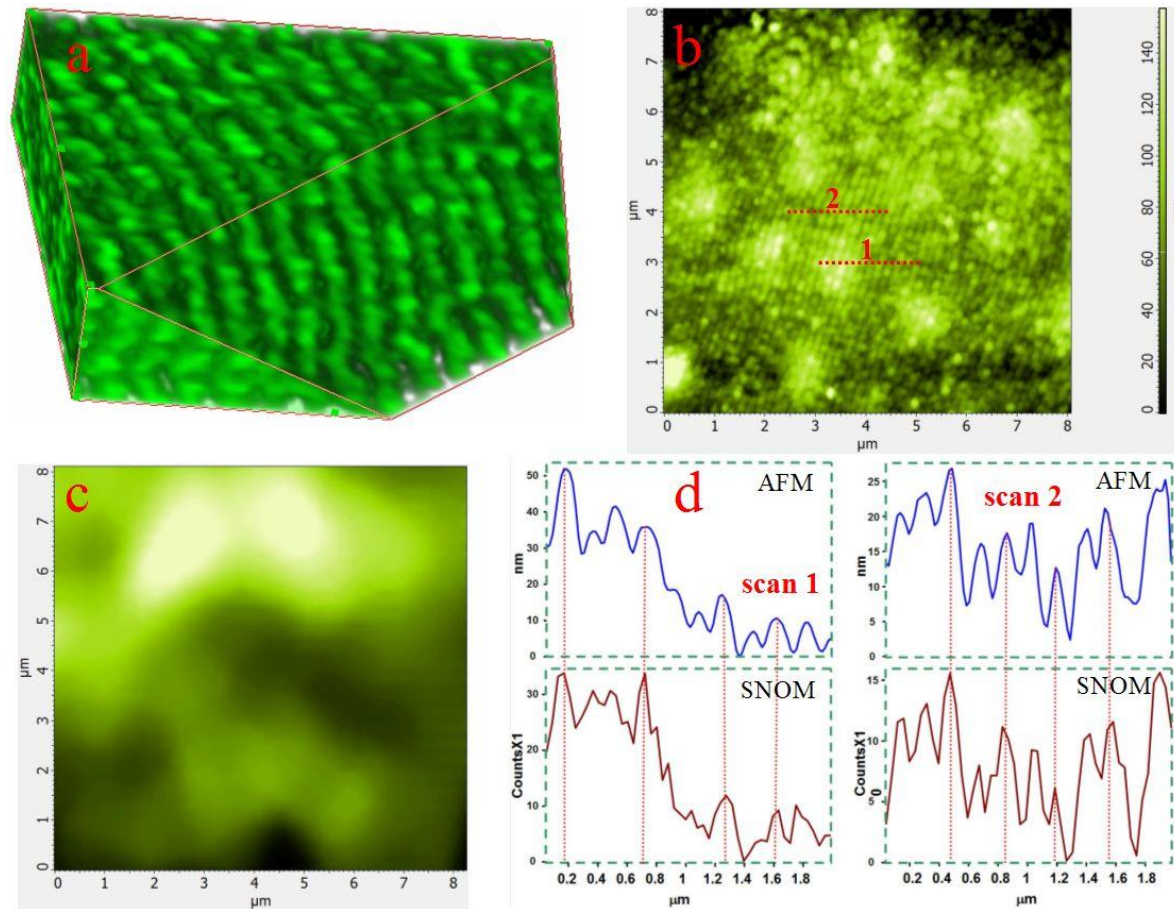


SNONT - 3D nanoscale multimodal characterization of nanomaterials with SPM and scanning near-field optical nanotomography.



SNONT - Results

SNOM is needed when the dimensions of optical features are below confocal resolution!



Correlation between nanoscale optical and morphological features of LC/QD materials using the 3D AFM and SNOM modes.

- a) 3D AFM
- b) 2D AFM of UMT-sliced sample. Lines 1 & 2 are crosssections for SNOM measurement
- c) Confocal fluorescent image of UMT-sliced sample.
- d) The comparison of AFM and SNOM crosssections from lines 1 & 2 on panel b.
Images courtesy of K.E.Mochalov, Institute of Bio-organic Chemistry RAS

Scientific publications for our technology

- 1) A. E. Efimov, H. Gnaegi, R. Schaller, W. Grogger, F. Hofer and N. B. Matsko, Analysis of native structure of soft materials by cryo scanning probe tomography, **Soft Matter**, 2012, 8, 9756, DOI:10.1039/c2sm26050f
- 2) K. E. Mochalov; A. Yu. Bobrovsky; V. A. Oleinikov; A. V. Sukhanova; A. E. Efimov; V. Shibaev; I. Nabiev, Novel cholesteric materials doped with CdSe/ZnS quantum dots with photo- and electro-tunable circularly polarized emission, **Proc. SPIE**, 2012, 8475, Liquid Crystals XVI, 847514
- 3) K. E. Mochalov, A. E. Efimov, A. Bobrovsky, I. I. Agapov, A. A. Chistyakov, V. Oleinikov, A. Sukhanova, and I. Nabiev, Combined Scanning Probe Nanotomography and Optical Microspectroscopy: A Correlative Technique for 3D Characterization of Nanomaterials, **ACS Nano**, 2013, DOI: 10.1021/nn403448p
- 4) Bobrovsky, A., Mochalov, K., Oleinikov, V., Sukhanova, A., Prudnikau, A., Artemyev, M., Shibaev, V., Nabiev, I. Optically and electrically controlled circularly polarized emission from cholesteric liquid crystal materials doped with semiconductor quantum dots. **Advanced Materials**, 2012, DOI: 10.1002/adma.201202227
- 5) A. Alekseev, D. Chen, E. E. Tkalya, M. G. Ghislandi, Yu. Syurik, O. Ageev, J. Loos, and G. de With Local Organization of Graphene Network Inside Graphene/Polymer Composites **Adv. Funct. Mater.** 2012, 22, 1311–1318
- 6) V. Mittal and N. B. Matsko, Tomography of the Hydrated Materials, in **Analytical Imaging Techniques for Soft Matter Characterization, Engineering Materials**, Springer-Verlag Berlin Heidelberg, 2012, pp. 85-93
- 7) A. Efimov; H. Gnaegi; V. Sevastyanov; W. Grogger; F. Hofer; N. Matsko, Combination of a cryo-AFM with an ultramicrotome for serial section cryo-tomography of soft materials - **Proceedings 10th Multinational Congress on Microscopy 2011** SEP 4-9, 2011; Urbino, ITALY. pp.707-708
- 8) N. B. Matsko, J. Wagner, A. Efimov, I. Haynl, S. Mitsche, W. Czapek, B. Matsko, W. Grogger, F. Hofer, Self-Sensing and – Actuating Probes for Tapping Mode AFM Measurements of Soft Polymers at a Wide Range of Temperatures, **Journal of Modern Physics**, 2011, 2, pp. 72-78
- 9) A. Alekseev, A. Efimov, K. Lu, J. Loos. Three-dimensional electrical property reconstruction of conductive nanocomposites with nanometer resolution, **Advanced Materials**, Vol. 21, 48 (2009), pp. 4915 – 4919
- 10) A. Efimov, V. Sevastyanov, W. Grogger, F. Hofer, and N. Matsko. Integration of a cryo ultramicrotome and a specially designed cryo AFM to study soft polymers and biological systems, **MC2009, Vol. 2: Life Sciences**, p. 25, Verlag der TU Graz 2009.
- 11) A. E. Efimov, A. G. Tonevitsky, M. Dittrich & N. B. Matsko. Atomic force microscope (AFM) combined with the ultramicrotome: a novel device for the serial section tomography and AFM/TEM complementary structural analysis of biological and polymer samples. **Journal of Microscopy**, Vol. 226, Pt 3, June 2007, pp. 207–217